AD-A049 946 SCHOOL OF AEROSPACE MEDICINE BROOKS AFB TEX F/G 6/18
CORNEAL DAMAGE THRESHOLDS FOR INFRARED LASER EXPOSURE: EMPIRICA--ETC(U)
DEC 77 D E EGBERT, E F MAHER

UNCLASSIFIED SAM-TR-77-29 NL

| OF |
AD A049946

END
DATE FILMED
3-78
DDC

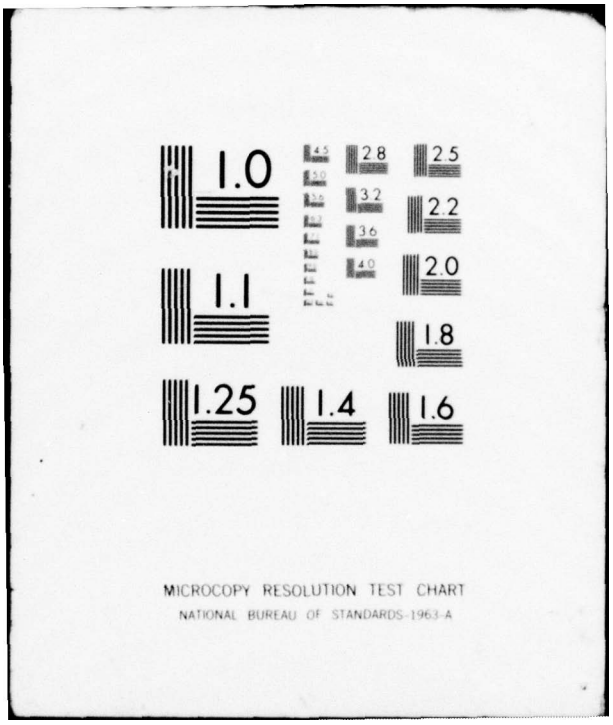
1.0
1.1
1.25
1.4
1.6
2.8
3.2
3.6
4.0
2.5
2.2
2.0
1.8
MICROCOPY RESOLUTION TEST CHART
NATIONAL BUREAU OF STANDARDS-1963-A

Report SAM-TR- 77-29

CORNEAL DAMAGE THRESHOLDS FOR INFRARED LASER EXPOSURE: EMPIRICAL DATA, MODEL PREDICTIONS, AND SAFETY STANDARDS

David E. Egbert, Captain, USAF

Edward F. Maher, Captain, USAF, BSC

December 1977

Final Report for Period April 1975-June 1977

Approved for public release; distribution unlimited.

USAF SCHOOL OF AEROSPACE MEDICINE
Aerospace Medical Division (AFSC)
Brooks Air Force Base, Texas 78235

NOTICES

This final report was submitted by personnel of the Laser Effects Branch, Radiation Sciences Division, USAF School of Aerospace Medicine, AFSC, Brooks Air Force Base, Texas, under job order 7757-02-52.

When U.S. Government drawings, specifications, or other data are used for any purpose other than a definitely related Government procurement operation, the Government thereby incurs no responsibility nor any obligation whatsoever; and the fact that the Government may have formulated, furnished, or in any way supplied the said drawings, specifications, or other data is not to be regarded by implication or otherwise, as in any manner licensing the holder or any other person or corporation, or conveying any rights or permission to manufacture, use, or sell any patented invention that may in any way be related thereto.

This report has been reviewed by the Information Office (OI) and is releasable to the National Technical Information Service (NTIS). At NTIS, it will be available to the general public, including foreign nations.

This technical report has been reviewed and is approved for publication.

David E Egbert

DAVID E. EGBERT, Captain, USAF
Project Scientist

Everett O. Richey

EVERETT O. RICHEY, M.S.
Supervisor

Robert G McIver

ROBERT G. MCIVER
Brigadier General, USAF, MC
Commander

UNCLASSIFIED

SECURITY CLASSIFICATION OF THIS PAGE *(When Data Entered)*

REPORT DOCUMENTATION PAGE

READ INSTRUCTIONS BEFORE COMPLETING FORM

1. REPORT NUMBER: SAM-TR-77-29	2. GOVT ACCESSION NO.
3. RECIPIENT'S CATALOG NUMBER	
4. TITLE *(and Subtitle)*: CORNEAL DAMAGE THRESHOLDS FOR INFRARED LASER EXPOSURE: EMPIRICAL DATA, MODEL PREDICTIONS, AND SAFETY STANDARDS	5. TYPE OF REPORT & PERIOD COVERED: Final Report, April 1975- June 1977
	6. PERFORMING ORG. REPORT NUMBER
7. AUTHOR(s): David E. Egbert, Edward F. Maher	8. CONTRACT OR GRANT NUMBER(s)
9. PERFORMING ORGANIZATION NAME AND ADDRESS: USAF School of Aerospace Medicine (RZL), Aerospace Medical Division (AFSC), Brooks Air Force Base, Texas 78235	10. PROGRAM ELEMENT, PROJECT, TASK AREA & WORK UNIT NUMBERS: 62202F, 7757 02
11. CONTROLLING OFFICE NAME AND ADDRESS: USAF School of Aerospace Medicine (RZL), Aerospace Medical Division (AFSC), Brooks Air Force Base, Texas 78235	12. REPORT DATE: Dec 77; 13. NUMBER OF PAGES: 61, 64p.
14. MONITORING AGENCY NAME & ADDRESS *(if different from Controlling Office)*	15. SECURITY CLASS. *(of this report)*: Unclassified; 15a. DECLASSIFICATION/DOWNGRADING SCHEDULE

16. DISTRIBUTION STATEMENT *(of this Report)*

Approved for public release; distribution unlimited.

17. DISTRIBUTION STATEMENT *(of the abstract entered in Block 20, if different from Report)*

18. SUPPLEMENTARY NOTES

19. KEY WORDS *(Continue on reverse side if necessary and identify by block number)*

Corneal damage thresholds	Corneal epithelium
Laser safety standards	Steam formation
Thermal modeling	Corneal stroma
IR lasers	Corneal perforation

20. ABSTRACT *(Continue on reverse side if necessary and identify by block number)*

Experimental damage threshold data for corneal injury from infrared lasers are compared with thermal model predictions of temperature rise, lesion radius, and damage threshold using several damage criteria. The functional dependence of the threshold exposure upon damage end-point, damage criteria, absorption coefficient, beam radius, exposure duration, and damage site is determined. Experimental and predicted thresholds are compared to the ANSI Z136.1-1976 laser safety standard. Similar analysis with the thermal model for applications such

DD FORM 1 JAN 73 1473 A EDITION OF 1 NOV 65 IS OBSOLETE

UNCLASSIFIED

SECURITY CLASSIFICATION OF THIS PAGE *(When Data Entered)*

317 000

20. ABSTRACT (Continued)
as photokeratoplasty or corneal and lenticular spectroscopy can yield alternative approaches to either maximize or avoid thermal effects often inherent in such research.

PREFACE

We express appreciation for the excellent support of the Laser Effects Branch, Radiation Sciences Division, and the Biometrics Division of the USAF School of Aerospace Medicine. The assistance and discussion with R. G. Allen, E. L. Bell, R. C. McNee, K. A. Toth, and S. M. Kane of USAFSAM and A. N. Takata of IIT Research Institute of Chicago, Illinois, were particularly significant. We are also indebted to G. W. Mikesell, Jr. of USAFSAM and B. E. Stuck of Letterman Army Institute of Research, Presidio, California, for helpful discussions and the use of their unpublished data.

TABLE OF CONTENTS

LIST OF ILLUSTRATIONS

LIST OF TABLES

CORNEAL DAMAGE THRESHOLDS FOR INFRARED LASER EXPOSURE: EMPIRICAL DATA, MODEL PREDICTIONS, AND SAFETY STANDARDS

INTRODUCTION

Current infrared (IR) laser safety standards (1, 2, 4, 5, 38) are based upon the threshold dose for a minimal visible lesion in the corneal epithelium, a tissue which heals within a few days. The safety standards are dependent only upon exposure duration. Presumably threshold dependence upon wavelength, beam size, or other damage end-points is accounted for by conservative standards.

The objective of this study was to develop a basis for IR laser safety standards which would incorporate wavelength and beam size dependence and consider other damage end-points. This would permit more realistic hazard evaluations and safety control measures. The commonly used lasers emitting at wavelengths greater than 1.4 μm are: CO_2 at 10.6 μm, CO at about 5 μm, HF or DF at 2-4 μm, holmium at 2.06 μm, and erbium at 1.54 μm. They have varied applications in communication, reconnaissance, and materials processing. A great variety of potential exposure conditions exist in terms of the duration, wavelength, beam distribution, and beam size.

To evaluate the hazards of these IR laser systems with exposures different from previous experimental studies, it is necessary to know the damage threshold levels and establish safety standards. An analysis of theoretical predictions of damage thresholds and experimental data lends support to portions of the current laser safety standards; however, it also indicated some deficiencies. The results demonstrate the utility of thermal model predictions both to provide a broader basis for IR safety standards and to optimize the results of clinical or related research applications of IR laser systems.

Three damage end-points were considered: minimal epithelial lesions, stromal collagen fiber shrinkage or opacities, and epithelial vaporization. The corneal stroma in some instances is about as sensitive to IR laser exposures as the epithelium, and stromal changes can have a more chronic effect upon visual function than those involving the epithelium alone (27, 45). Likewise the acute effects from corneal perforation and steam formation are considered, since they have threshold doses only a factor of ten above those for minimum epithelial lesions. Because of the scatter in the threshold data, all of these effects must be considered in the IR laser safety standards.

Model predictions of the threshold dose and temperature histories were made for each of the three damage end-points. The lesion radius was also predicted for minimal epithelial lesions. These model predictions were made for experimental exposure conditions and exposure conditions representative of corneal hazards over the entire range of

pertinent IR wavelengths (between 1 μm and 1000 μm), exposure durations (1 ns to 8 hours), and beam radii (10 μm to 1 cm).

Damage threshold predictions from the corneal model and experimental data were then used to show the functional dependence of the threshold radiant exposure (for a particular damage end-point) upon exposure duration, wavelength, and beam size. The experimental and predicted thresholds were compared with current safety standards of the American National Standards Institute (ANSI), and the implications for laser safety, clinical, and related research applications for IR lasers were noted.

BACKGROUND

Current standards are based on the damage threshold doses determined for CO_2 lasers at 10.6 μm for exposure durations longer than 1 ms and upon related theoretical model calculations. From these damage threshold studies various governmental agencies (1, 4, 5, 38) and the ANSI (2) established IR safety exposure standards for potential exposure conditions ranging from 1 ns to 8 hours for wavelengths of 1.4 to 1000 μm.

A summary of the experimental damage threshold exposure conditions reported in the literature is presented in Tables 1, 2, and 3 for the three damage end-points (minimum visible epithelial lesion, stromal collagen shrinkage or opacities, and epithelial vaporization, respectively). The ANSI standards are also listed in the tables. Listed in Table 4 are the various lasers, specific wavelengths, and associated absorption coefficients used for the experimental exposures. The experimental threshold radiant exposures and current ANSI standards are plotted in Figure 1 as a function of exposure duration. This summary includes recent data not contained in previous reviews of corneal damage thresholds from IR lasers (3, 14, 62, 63, 70).

The following damage threshold criteria were used to tabulate the data in Tables 1-3. The threshold criterion used for a minimum corneal epithelial lesion was the appearance of a relatively faint, greyish-white, stippled area (presumably light scattering from an opacity, coagulation, edema, or infiltrates), usually in the epithelium but possibly in the stroma, which occurs within 1 or 2 hours postexposure. A subsequent epithelial sloughing or depression which exhibits mild fluorescein staining may also be observed. Healing occurs within a few days without permanent scarring.

The threshold criterion used for stromal collagen shrinkage or a stromal opacity was the appearance of a distinct area of light scattering (clouding, opacity, coagulation), observed in the stroma within about 1 hour postexposure and associated with subsequent thickening, change of curvature (flattening, band keratopathy), or scarring of the cornea.

The threshold criterion used for epithelial steam formation or corneal perforation was severe stromal injury with crater formation, charring, and bubbles in the stroma or perforation of the cornea into the aqueous immediately after exposure.

The experimental exposure conditions were not always completely described, thus requiring some assumptions about beam size and distribution, and other factors as indicated by the footnotes in the tables.

Use of a theoretical model to predict damage threshold exposures and their effects assumes a degree of confidence in the mode. However, large variances (or inadequate data) exist among reported values for significant model input parameters such as thermal conductivity (8, 69); specific heat (8); absorption coefficients (6, 12, 16, 17, 33, 37, 50, 57-59, 79); initial temperatures (25, 44, 45, 46, 60); ocular media layer thicknesses (15, 47, 69); damage rates (9, 26, 35, 36, 48, 55, 68. 75, 76); critical temperatures; and latent heats of transformation. In many cases, data do not exist for a specific ocular layer and characteristics of similar tissue or substance are selected to represent it. Likewise large variances exist among experimental threshold exposures because of the wide variety of threshold criteria, incompletely specified exposure conditions, and the extent, nature, history, and location of their effects. With the problems that exist, agreement in functional dependence of the model and experiment is the best one might expect. However, the model can be used to determine the functional dependence of the many interrelated variables. After a given functional relationship is defined from theoretical considerations model predictions can be normalized to accepted experimental values.

THEORY

Previous theoretical studies (9, 13, 34, 43, 52-54, 71) have calculated corneal temperature rises as solutions of a one- to three-dimensional heat diffusion equation. It was assumed that damage occurred when a threshold temperature rise was exceeded, or when a damage integral exceeded a specified value. The thermal model used here was adapted from that of Mainster et al. (43) by Takata et al. (69) of IIT Research Institute (IITRI). The IITRI model predicts the threshold dose and the lesion radii and depth, in addition to the temperature rise history, as a function of axial and radial position. It models: (a) the incident radiation as a function of its duration, wavelength, divergence, beam size, and its axially symmetric intensity distribution; (b) the irradiated tissue as a function of its anatomical, optical, and thermal properties for six homogeneous layers; and (c) the thermal damage mechanism as a function of damage rates of critical peak temperatures.

The temperature rise history is calculated via the heat diffusion equation:

$$(1/\rho c)\ (dT/dt) = A+K\nabla^2 T \qquad (1)$$

where the source term, A, assumes Lambert absorption.

$$A = -d/dz\,[H_0(r,t,)\exp(-\alpha z)] = \alpha H_0(r,t)\exp(-\alpha z) \qquad (2)$$

where $H_0(r,t)$ is the spatial beam distribution, z is the axial depth, and α is the absorption coefficient. Note the explicit dependence of the source term upon the absorption coefficient in equation 2.

The IITRI model can calculate the thresholds directly from the temperature histories via the damage rate integral

$$\Omega = \int C1\ \exp(C2/T(t))dt = 1 \qquad (3)$$

only for the minimum visible epithelial lesion end-point. The rate constants, C1 and C2, have not been determined for the other end-points. Thresholds for all three damage end-points can be calculated from the IITRI model temperature histories using the critical peak temperature (CPT) as a damage criterion.

The CPT is the sum of the peak temperature rise and the initial temperature, T_0, of 35°C (25, 45). For a minimum visible epithelial lesion an empirical CPT was derived as a function of exposure duration from temperature predictions for the experimental threshold doses listed in Table 1. (The values for the empirical CPTs are presented in the "Results.")

The CPTs used to predict collagen fiber shrinkage in the stroma and epithelial steam formation are derived from theoretical phase changes. The energy absorption required for the phase change was modeled for both adiabatic and nonadiabatic absorption.

The adiabatic CPT for stromal collagen shrinkage is 56°C and the nonadiabatic CPT is 61°C. Some theories indicate that collagen shrinkage is like a melting phenomenon with a definite melting point estimated at about 56°C and a latent heat of transformation of 25 cal/g of collagen (28, 32). About 20% of the stroma is collagen and 80% is water by weight (56). Assuming a 1°C temperature rise is predicted by the model per cal/g absorbed, the additional 25 cal/g of collagen is equivalent to an additional 5°C temperature rise--hence 61°C.

The nonadiabatic CPT for steam formation is 639°C. It is the sum of the 100°C boiling temperature at normal atmospheric pressure, and 539°C derived from the 539 cal/g required for the latent heat of vaporization, assuming a 1°C temperature rise is predicted for each cal/g absorbed. The nonadiabatic CPT can be interpreted as the temperature that must be predicted by the model to represent a phase transition.

The adiabatic estimate of the threshold radiant exposure for collagen shrinkage or steam formation is the sum of the radiant exposure required to achieve the transition temperature (adiabatic CPT), and the radiant exposure on the cornea required for an adiabatic absorption of the latent

heat of transformation (5 or 539 cal/cm^3, respectively). The damage threshold estimates from the adiabatic and the nonadiabatic CPT should bound the actual threshold value for the collagen shrinkage or steam formation.

For all the damage criteria just discussed a simple relationship exists between the threshold dose and the absorption coefficient because of the explicit dependence of the temperature rise upon the absorption coefficient in the heat diffusion equation. The threshold dependence upon wavelength then is defined by the complex relationship between the absorption coefficients and the wavelength. The ocular media are usually well represented by the water spectra for the wavelengths $\geq$1.4 μm. The water absorption spectrum between 1 and 1000 μm is plotted in Figure 2. Since several wavelengths can correspond to a given corneal absorption coefficient, the threshold predictions for a given absorption coefficient apply for all those wavelengths. This assumes that the absorption and reflectivity of the other ocular layers (principally the tear layer) corresponding to the various wavelengths having a common corneal absorption coefficient are not significantly different from the set of optical properties used for the model predictions. Corrections must be made for high reflectivities from the tear layer at wavelengths above 70 μm.

PROCEDURE

Model Predictions and Experimental Data

To establish a level of credence in the theoretical calculations, the thermal model predictions were compared to the experimental measurements listed in Tables 1-3. Lesion radii, temperature histories, and threshold radiant exposure levels were predicted and compared to experimental determinations. Lesion radii, r_ℓ, were predicted, based upon the damage integral criteria and the experimental lesion threshold exposure conditions. The relative lesion radius is the ratio of r_ℓ to σ, the 1/e beam radius. The mean of the relative lesion radii was calculated from the relative lesion radii predicted for 30 epithelial lesion exposure conditions.

The empirical CPT for minimum epithelial lesions was calculated from the equation of the line through the central peak temperatures as a function of exposure duration from the experimental conditions listed in Table 1. A linear regression in logarithmic coordinates was used to determine the exponential equation of the CPT line. This empirical CPT is not an estimate of a threshold peak temperature, but merely a convenient parameter relating the predicted peak temperature at the beam axis to the experimental threshold dose. Threshold peak temperatures would occur at the lesion radii. An estimate of the threshold peak temperature was calculated from the peak temperatures predicted at the mean lesion radius.

The threshold radiant exposures for the three thermal damage end-points were predicted from the temperature rise history and damage criteria already described. Two damage criteria were used with each end-point.

The average threshold from the two damage criteria was also calculated. The damage integral and an empirical CPT damage criterion were used for the minimum visible lesion end-point. The adiabatic and nonadiabatic CPTs were used for both collagen fiber shrinkage and steam formation end-points.

The CPT threshold predictions were based upon peaks in the temperature histories. Only temperature histories on the beam axis--either at the tear-epithelium interface, z = 6 μm, or at the anterior surface of the stroma, z = 66 μm--were considered in this study. The threshold predictions using the damage integral criterion were calculated from the entire temperature history, both on the beam axis and at the mean lesion radii, r_ℓ; at a depth of 6 μm.

For the nonadiabatic and empirical CPT criteria the threshold radiant exposures, $H(J/cm^2)$, were calculated from

$$H = (CPT-T_o)t/T_nS \qquad (4)$$

where CPT is the appropriate nonadiabatic or empirical critical peak temperature for a given damage end-point, T_o is the initial temperature in °C, t is the exposure duration in sec, T_n is the normalized peak temperature rise in °C/W predicted by the IITRI model at the damage site depth on the beam axis, and S is the 1/e area of the incident beam in cm^2.

For the adiabatic CPT criteria the threshold radiant exposures were calculated from

$$H = (CPT-T_o)t/T_nS + (4.186\ L\cdot\rho\ \exp(\alpha z)/\alpha\cdot(1-R)) \qquad (5)$$

where CPT is the phase transition temperature in °C, $L\cdot\rho$ is the latent heat of transformation-mass density product in cal/cm^3, α is the absorption coefficient in cm^{-1}, R is the tear layer reflectivity, and z is the coordinate of the damage site in cm. This adiabatic estimate is a decreasing function of the absorption coefficient until the exp (αz) factor begins to dominate the equation 5 as for large αz products. Because of the conduction of heat to the damage site during and after the exposure, which is ignored by the adiabatic approximation, the predicted threshold cannot increase with the absorption coefficient. For large αz products, the adiabatic estimate from equation 5 exceeds the nonadiabatic estimates, thus indicating that the adiabatic estimate is inappropriate. To avoid these problems the adiabatic threshold is set equal to the least of either its minimum value (as a function of α) or the associated nonadiabatic threshold estimate. These instances are indicated in the tables of the threshold predictions.

The corneal anatomical and thermal properties (including the damage criteria) used in all the model predictions are listed in Table 5. The optical properties of the cornea and adjacent ocular media which were used in the model are from Boettner and Dankovic (6) or those of water (50, 59, 79). See Figure 2.

Damage Thresholds, Their Functional Dependence and Safety Standards

Damage thresholds were predicted over the range of exposure parameters listed below to establish the functional relationships among the thresholds, the end-points, the damage criteria, and the exposure conditions. The same procedures were used as described above for the experimental exposure conditions except all threshold predictions were limited to the beam axis.

The damage thresholds were calculated from the IITRI temperature rise histories for 0.0707 cm beam radius (1/e) for the three damage end-points (minimum epithelium lesions, stromal collagen fiber shrinkage, and epithelial vaporization). These thresholds were calculated as a function of the corneal absorption coefficient (at 25 values between 0.7 and 12395 cm^{-1}) and exposure duration (between 10^{-8} and 10^{2} sec). They were also calculated for an absorption coefficient of 817 cm^{-1} as a function of (1/e) beam radius between 10^{-3} and 1.0 cm and exposure duration. The functional dependence of the damage thresholds was determined from the plots and tables of the predicted threshold radiant exposure as a function of the various parameters (exposure duration, absorption coefficient, beam radius, and the criterion and end-point for damage). The wavelength dependence was derived from the threshold dependence upon the absorption coefficients.

The relative threshold sensitivity was calculated for the wavelengths of the common IR lasers in the 1.4 - 1000 μm wavelength range. The relative threshold sensitivity is defined as the ratio of the threshold for the highest absorption coefficient (i.e., lowest threshold) in the 1.4 - 1000 μm range to that for any given absorption coefficient. The minimum threshold occurs at about 2.9 μm (12395 cm^{-1}). The relative sensitivity was calculated for the three damage end-points.

The experimental damage threshold and model predictions were compared to ANSI laser exposure standards for the three damage end-points. The safety margins, i.e., the ratios of the threshold predictions to the ANSI standards, were calculated as a function of absorption coefficient, beam radius, and exposure duration. The functional dependence of the damage thresholds and ANSI standards were compared.

RESULTS

Model Predictions and Experimental Data

The model predictions for the experimental exposure conditions are listed in Tables 1 to 3 for the minimum epithelial lesion, stromal collagen shrinkage or opacities, and epithelial vaporization damage end-points, respectively. The model predictions for minimum epithelial lesions include the relative lesion radius (relative to the 1/e beam radius), the peak temperature rise on the beam axis, the threshold prediction from the damage integral at the mean relative lesion radius, $H_{\ell di}(\bar{r}_{\ell})$, and the average

threshold prediction on the beam axis, $H_{\ell a}(0)$. The average threshold predictions are the average of the predictions from the damage integral, $H_{\ell di}$, and the empirical CPT criteria, $H_{\ell c}$. The mean relative lesion radius, $\bar{r}_\ell$, at a depth of 6 μm was 0.76 times the 1/e beam radius, $r = 0.76\sigma$, with a 90% confidence interval of (0.70 to 0.82) σ. This mean relative lesion radius corresponds to the 0.56 relative intensity point.

Listed in Table 1 are the predicted peak temperature rises on the beam axis resulting from radiant exposures equal to $H_{\ell e}$, the experimental lesion thresholds. The exponential equation of the line through the resultant temperatures as a function of the exposure durations is the empirical CPT for epithelial lesions:

$$CPT = 79.6t^{-0.0152} \tag{6}$$

Listed in Table 6 are representative values of the empirical CPT, and temperature rise, ΔT, for selected exposure durations, t.

An estimate of the minimum lesion threshold peak temperature, TPT, is given by the regression line through peak temperatures at the mean relative lesion radii, 0.76σ.

$$TPT = 61.2t^{-0.0116} \tag{7}$$

In Table 7 are listed representative values as a function of exposure duration, t. On the average, the peak temperature rise at the mean lesion radius was 0.56 of that on the beam axis.

Presented in Table 8 is a comparison of the theoretical and experimental estimates of lesion radii, temperature rises, and threshold radiant exposures for minimum epithelial lesions and the ANSI laser exposure standards. The experimental threshold data for minimum epithelial lesions are plotted in Figure 3 for comparison to model predictions. The model predictions in Figure 3 are not the individual predictions from Table 1, but the average predicted lesion thresholds, $H_{\ell a}$ (0), for corneal absorption coefficients of 11, 200, and 1000 cm^{-1} for a nominal beam radius (σ = 0.0707 cm). These three absorption coefficients represent the erbium (1.54 μm at ≈11 cm^{-1}), DF (3.5 to 4 μm at about 200 cm^{-1}), and HF and CO_2 (2.5 to 3.0 μm and 10.6 μm at greater than 1000 cm^{-1}) laser exposures.

Listed in Tables 2 and 3 are the model predictions for the experimental exposure conditions which result in stromal collagen shrinkage or opacities and epithelial vaporization, respectively. The model predictions include the peak temperature rises on the beam axis and the average thresholds from the two damage criteria for each end-point, H_{sa} and H_{va}, respectively. The comparison among the various threshold estimates and ANSI exposure standards is presented in Tables 9 and 10 for stromal damage and epithelial vaporization, respectively.

The experimental thresholds for stromal damage are compared to the average threshold predictions for absorption coefficients of 11 and 1000 cm^{-1} at the nominal beam radius in Figure 4. Likewise, experimental

thresholds for epithelial vaporization are compared to average threshold predictions for absorption coefficients of 1000 cm^{-1} in Figure 5.

Damage Thresholds, Their Functional Dependence and Safety Standards

The average threshold radiant exposure predictions for each of the three damage end-points are presented in Tables 11-13 as a function of the absorption coefficients and the exposure duration for a nominal 1/e beam radius (σ = 0.0707 cm). Likewise, Tables 14-16 contain the average threshold predictions as a function of beam radius and exposure duration for absorption coefficient of 817 cm^{-1}.

Selected threshold radiant exposure values listed in these tables are shown in Figures 6-19. These plots show the relationship of the absorption coefficient, wavelength, beam radius, and exposure duration to the damage thresholds for the three damage end-points and the several damage criteria.

The dependence of damage thresholds on the absorption coefficient and damage criterion for $\leq 10^{-4}$, 1.0, and 10^{2} sec exposures is presented in Figures 6, 7, and 8 for the three damage end-points (minimum epithelial lesion, stromal collagen shrinkage, and epithelial vaporization, respectively). The thresholds are plotted for each of the two damage criteria used for each end-point. The averages of the two threshold estimates for each damage end-point are plotted in Figures 9-11 as a function of wavelength for $\leq 10^{-4}$, 1.0, and 10^{2} sec exposures. The threshold dependence upon beam radius is presented in Figures 12-14 for the three damage end-points. The average thresholds are plotted as a function of a beam radius for $\leq 10^{-4}$, 1.0, and 10^{2} sec exposures.

Shown in Figures 15-19 are the threshold dependence upon the exposure duration and damage end-point for the principal IR laser wavelengths for corneal hazards. The average thresholds for each of the three damage end-points for a 0.0707 cm 1/e beam radius are plotted as a function of exposure duration. Erbium lasers are represented by an absorption coefficient of 11 cm^{-1} in Figure 15; holmium lasers, by 41 cm^{-1} in Figure 16; DF and CO lasers, by 200 cm^{-1} in Figure 17; CO_2 and some HF laser lines, by 1000 cm^{-1} in Figure 18; and HF laser lines around 3 μm, by 12395 cm^{-1} in Figure 19.

Listed in Table 17 are the predicted relative threshold sensitivity for the common IR laser wavelengths above 1.4 μm. Table 18 lists the ratio of the predicted thresholds to the ANSI laser exposure standards, the safety margins, as a function of absorption coefficient and exposure durations. Likewise, Table 19 lists the same ratio as a function of beam radius and exposure duration for an absorption coefficient of 817 cm^{-1}. ANSI standards are shown in Figures 15-19 for comparison to model predictions.

DISCUSSION

Model Predictions and Experimental Data

The agreement between damage threshold predictions and experimental data in both their functional dependence and the actual exposure levels can be seen in Figures 3-5. This agreement is better than might be expected considering the potential problems already discussed (in "Background"). Thermal predictions are well within the probable scatter of the data, if the scatter is that which is observed about the 1000 cm^{-1} line for the HF and CO_2 exposures (Figures 3-5). The differences between the predicted and experimental thresholds for the CO_2 exposures at 900 sec and 1800 sec can be attributed to the differences in beam size for the experimental and predicted threshold exposure conditions (0.52 and 0.0707 cm, respectively).

The comparison of the thermal model predictions to the experimental measurements has yielded the following which establish a level of confidence in the model predictions: The average threshold predictions (from the two damage criteria) for minimum epithelial lesions, stromal collagen shrinkage, and epithelial vaporization were on the average 0.8, 0.4, and 1.2 of the experimental radiant exposures, respectively. Although there are no experimental measurements of the lesion radii or peak temperatures for the experimental conditions in Tables 1-3, the predictions for lesion radii are not unreasonable and the prediction for the temperature rises agree with earlier studies. The mean relative lesion radius, $r_\ell = 0.76\sigma$, for minimum epithelial lesions is reasonable, since the temperature rises predicted at this radius (Table 7) compare favorably with estimates for enzyme and protein denaturation (51).

The model predictions of the temperature rises for minimum epithelial lesions and empirical CPT derived from them (Tables 6 and 7) are a few degrees higher than those reported in the literature (43, 54, 72). However, this increase can be explained by the differences in the parameter values used for the tear layer and corneal absorption coefficient.

The temperature rise predictions for experimental stromal effects were quite erratic, but were usually much above the collagen melting temperature (26°C above an initial temperature of 35°C). (See Table 2.) However, the measurements of the collagen melting temperatures were made for steady-state exposures to heat. For short exposures (Table 2) higher temperature rises would be expected.

The predicted temperature rises for epithelial vaporization are lower than the nonadiabatic criteria (604°C), ranging from a 230°C to a 380°C temperature rise.

The threshold radiant exposure predictions for the minimum epithelial lesions were normalized to experimental values via the empirical CPT and damage integral criteria. The effect of this normalization is evident in the comparison of experimental and theoretical threshold estimates (Tables 1 and 8). Likewise, the appropriateness of the theoretical assumptions for

stromal and epithelial vaporization thresholds can be judged from the same comparison (Tables 2 and 9, 3 and 10, respectively).

In the following analysis the values reported are averages of the experimental exposures. The ratio of the threshold predictions for minimum epithelial lesions, $H_{\ell c}$ (via the empirical CPT) to $H_{\ell di}$ (via the damage integral)--was on the average 1.7. Their mean was 0.8 of the experimental value. Likewise, the damage integral prediction at the mean lesion radius, $H_{\ell di}(\bar{r}_{\ell})$, was 1.03 times the experimental value. While the ratio of the two threshold estimates from the stroma was 1.2, their mean was only 0.4 of the experimental value. For epithelial vaporization, the ratio of the two threshold estimates was 6.2; but their mean was 1.2 times the experimental value. The underestimation of the stromal thresholds is due to the assumption of a collagen shrinkage at a fixed steady-state temperature independent of the exposure duration. If stromal CPTs increased with shorter exposures, as the lesion CPT do, stromal threshold predictions would improve. The better overall agreement of threshold predictions for the epithelial damage (minimum lesions and vaporization) can be primarily attributed to the use of empirical damage criteria and a well-defined phase change.

The favorable comparison of the thresholds derived from the damage integral and those from the simple CPT criteria gives credence to the use of the CPT concept as a damage criterion. This concept has been assumed in the literature for some time; i.e., that damage occurs when some critical or threshold temperature is reached. However, it should be noted that the CPTs used in this study were indeed the temporal peak temperatures and not just the temperatures at the end of the exposure. They occurred up to tens of milliseconds after the end of the exposure, depending upon the spatial temperature distributions and the radial and axial distance of the damage site from the spatial peak temperatures.

In summary, the good agreement of the model predictions with the experimental data provides a degree of validation for the model and the damage thresholds predicted by it over a wide range of exposure conditions for three damage end-points.

Damage Thresholds and Their Functional Dependence

The functional dependence of the damage thresholds can be separated into the dependence upon the damage end-point and criteria; and the dependence upon the absorption coefficient, beam radius, exposure duration, and damage site. The CPT-rise, CPT-T_o, (Eqs. 4 and 5) depends only upon the damage end-point and the criteria. The $(t/T_n S)$ factor and the latent heat term depend on the absorption coefficient, α; beam radius, σ; exposure duration, t; and damage site (r, z). For a given set of values for α, σ, t, r, and z, the thresholds were proportional to the CPT-rise for the appropriate end-point. The lesion thresholds calculated via the damage integral, $H_{\ell di}$, were proportional to some effective CPT-rise (Fig. 6). The CPT-rises for minimum epithelial lesions and stromal collagen shrinkage were approximately

the same order of magnitude, while those for epithelial vaporization were about a factor of ten above the CPT-rise for the other two end-points (Table 5). This relationship (i.e., $H_{\ell a} \simeq H_{sa} = H_{va}/10$) among the threshold radiant exposures for the three damage end-points can be seen in Figures 15-19.

The functional dependence of threshold radiant exposures for the stromal damage end-point changes from that for epithelial damage. This change is due to the differences in the absorption of the media and the conduction of heat at the depth of the site of damage. Thresholds increase with the depth of the damage site proportional to $\exp(\alpha z)/\alpha$ (for exposures $\lesssim 10^{-2}$ sec), and the conductivity. Hence, as the absorption coefficient, α, increases from about 10 cm^{-1} (for exposures $\lesssim 10^{-2}$ sec) stromal thresholds increase to about a factor of 6 relative to minimum epithelial lesion thresholds at the maximum absorption coefficient. Since minimum epithelial lesions and epithelial vaporization have a common damage site depth, they exhibit a similar threshold functional dependence.

For a given damage end-point and criteria, damage thresholds were inversely proportional to the lower absorption coefficients and independent of them at high absorption coefficients. The break points for the epithelial thresholds are: 1000 cm^{-1} for $\lesssim 10^{-4}$ sec; 100 cm^{-1} for $\lesssim 1.0$ sec, and 10 cm^{-1} for 10^2 sec exposures. Likewise, for stromal thresholds, the break points are 100 cm^{-1} for $\lesssim 1.0$ sec, and 10 cm^{-1} for 10^2 sec exposures. (See Figures 6-8.) This relationship follows from the direct absorption being proportional to $\alpha \exp(-\alpha z)$. When the exponential factor is near unity, as for low α values, sufficient energy is transmitted to the damage site to cause temperatures proportional to α (and thresholds inversely proportional to it). When the exponential factor is near zero, as for high absorption coefficients, the energy arriving at the damage site is primarily from conduction and independent of α.

For a given damage end-point and criteria, damage thresholds were almost inversely proportional to the square of the beam radius for small radii and independent of it for larger radii. The limits of a one dimensional heat flow model (23) indicated that the temperature rise (or threshold exposure) was independent of the beam radius for radii greater than $\sqrt{4Kt/\rho c} \simeq 0.1 \sqrt{t}$ (e.g., 10^{-2} cm radius for $t = 10^{-2}$ sec and 1 cm radius for 10^2 sec). These break points are evident in Figures 12-14. The beam size dependence for small radii is explained by radial (in addition to axial) heat diffusion.

For a given damage end-point and criteria, damage thresholds were independent of exposure duration for short exposures (10^{-2} to $\lesssim 10^{-4}$ sec), and directly proportional to it for longer exposures ($\simeq 1$ sec). The break points are dependent upon the absorption coefficients and the depth of the damage site (Figures 15-19).

In Figures 9-11 the thresholds for the three damage end-points demonstrate the complex functional dependence upon wavelength in comparison to that upon the absorption coefficient in Figures 6-8. One can also note

the smoothing effect that conduction has on the wavelength dependence at the greater exposure durations or depths (stromal vs. epithelial). The wavelength dependence of the thresholds can be significant between 1.4 μm (adjacent to the first minimum on the left in Figures 9-11) and 1000 μm. The relative sensitivity for the common IR laser wavelengths is listed in Table 17 for exposures less than 10^{-4} sec. Note the lack of sensitivity of the stroma to these wavelengths (or absorption coefficients). Even at "eye safe" wavelengths such as 1.54 μm, stromal thresholds are at most only a factor of 7 above the thresholds for most hazardous wavelengths. This factor may be compared with a factor of 55 for the epithelial effects.

Implications for Laser Safety Standards

Laser safety standards are based upon damage thresholds which are lowered by some factors to become safety standards. The safety factors account for variations in the threshold determinations and the inability, in some cases, or need to determine actual exposure conditions. Theoretically, some percentage (e.g., 99%) of normal persons exposed to the safety standard levels will not be injured. The acceptable percentage and degree of injury have not been defined. Current standards apparently are based on an intuitive estimate of an acceptable risk.

A safety factor of ten has often been assumed, usually without any attempted justification. Dunsky et al. (19) stated that for the visible wavelengths it included, "biologic variation among subjects; a cellular damage threshold occurring below the lowest visible damage threshold; uncertainties in data from different investigators; and the concern in extrapolating from rhesus monkeys to humans." Other safety factors have also been suggested. Sliney and Freasier (63) specified 0.1 W/cm^2 as a permissible exposure for up to several minutes for incidental exposures, but recommended a factor of 10 below it for long-term chronic exposures. They noted that daylight corneal exposure to the infrared is on the order of 10^{-3} W/cm^2. Some of the considerations for safety factors are very difficult to determine; however, the variation of the available threshold estimates can be determined. The variation of experimental data and theoretical predictions can be used as lower estimates for the safety factor. The variation in threshold values is due to biologic differences among individual subjects, different investigative techniques, and the use of subjective damage criteria. Other aspects of safety factors are not included, such as: concern for damage end-points with lower criteria, extrapolation from monkeys and rabbits to humans, chronic vs. acute exposures, or the seriousness of the result. Factors for each aspect, however, are not necessarily independent.

Epithelial lesion thresholds (experimental and theoretical) were estimated to be within factors of 3 to 9 of the actual threshold values. This estimate was derived from the following observations. On the average, individual experimental thresholds for $\lesssim 10^{-4}$ sec, 100 ms, and 500 ms exposures were within factors of 1.8, 1.2, and 1.3 of their means, respectively. The average model predictions, $H_{\ell a}$, for the experimental exposure conditions

were within a factor of 2.4 of all 35 experimental threshold estimates. Individual model predictions from the two damage criteria were within a factor of up to 2.0 of their means, $H_{\ell a}$.

Stromal threshold estimates were estimated to be within a factor of 6 of the actual threshold level. There were factors of up to 1.1 between individual experimental estimates and their mean for 1.0 sec exposures, a factor of up to 5 between average model predictions, H_{sa}, and the 13 experimental estimates, and a factor of up to 1.1 existed between model predictions from the two damage criteria and their means, H_{sa}.

Epithelial vaporization threshold values were estimated to be within a factor of 3 to 9 of actual threshold levels. A factor of up to 1.4 existed between individual experimental thresholds and their mean for 1 sec exposures; a factor of up to 1.6 between model predictions, H_{va}, and the 5 experimental estimates; and factors of up to 3.9 between model predictions of the two damage criteria and their means, H_{va}.

On the basis of this analysis, safety factors should not be less than 3 nor larger than about 10. These factors might decrease--if it were acceptable for less than 100% of the data to fall within the stated factors.

The safety margins for the experimental and the associated predicted thresholds for epithelial lesions, derived from data in Table 1, range from factors of 2.0 to 151. About 30% of these threshold estimates have safety margins of 5 or less, while 60-70% are factors of less than 10. The safety margins derived from data in Table 2 for experimental stromal thresholds ranged from factors of 3.5 to 45. Although most safety margins were at least 20 times ANSI standards, about 30% did have factors of less than 5. Model predictions for the stroma were all less than 20 times the ANSI standards. The experimental and predicted epithelial vaporization thresholds ranged from 41 to 115 times ANSI standards.

In Tables 18 and 19, safety margins for epithelial lesion predictions ranged from 4000 to as low as 3.6 times ANSI standards. Generally, the safety margins increased to factors of 100 and 1000 times ANSI standards as absorption coefficients decreased from 200 cm^{-1} and exposure durations decreased from about 10^{-2} sec; or as beam radii decreased from 10^{-2} cm for long exposures ($\geq$ 1.0 sec). Stromal threshold predictions in Tables 18 and 19 followed the same pattern as for minimal lesions, with larger safety margins except for exposures greater than about 10^{-2} sec. Then safety margins were about the same as for minimum lesions. Also, epithelial vaporization predictions and their safety margins were approximately a factor of ten above those for minimum lesions.

A region for concern, with respect to laser safety, is the area where safety margins approach the variance associated with the threshold estimates alone (i.e., factors of 3-10), particularly for permanent damage endpoints. Safety margins are between 3.6 and 24 (Tables 18 and 19) for absorption coefficients greater than 200 cm^{-1}, and exposures longer than

10^{-4} to 10^{-2} sec for epithelial lesions and stromal collagen shrinkage. For these conditions, threshold exposures which may fall below the mean estimate (but still within the expected variance) could be less than ANSI standards. It is suggested that either the standards should be lowered or at least the present degree of risk be defined. Stromal threshold estimates have essentially no greater safety margins than minimum epithelial lesions, except for absorption coefficients greater than 200 cm^{-1} for $\lesssim$ 10^{-4} sec exposures. The one end-point is entirely reversible within a few days, and the other may leave permanent scars and opacities. Thus the stromal effects warrant a greater margin of safety than is required for minimal epithelial lesions for exposures longer than 10^{-4} sec.

A second region for concern is where safety margins are excessive (>100), as exist for absorption coefficients $\lesssim$ 200 cm^{-1} for exposures $\lesssim$ 10^{-2} sec. Strict adherence to ANSI standards for excessive safety margins can easily restrict laser applications and cause the implementation of unnecessary and expensive safety measures. Experimental thresholds for erbium and DF at about 50 ns (Table 1) have thresholds 21 and 151 times ANSI standards. The erbium standards were increased by a factor of 100 (or the 21 would be 2100). The DF standards should also be increased. Likewise threshold predictions for holmium are up to 439 times ANSI standards (Table 18). However, rather than adjust each individual laser line as empirical data become available, a correction factor is suggested based on the absorption coefficient. A similar factor is used for the near ultraviolet or near infrared ANSI laser standards. Such a correction factor might be $F = 1000/\alpha$ for $\alpha(cm^{-1}) \leq 1000$ for exposures of less than $\leq 10^{-2}$ sec. Although ANSI standards are very conservative for beam radii of less than 10^{-2} cm, the problem is not considered significant. Such small beams are seldom used. When they do occur in research or other applications, there is justification for large correction factors to the basic ANSI standards.

Implications for Research and Clinical Applications

The model predictions presented can provide an estimate of the expected results from corneal irradiation from IR lasers for research or for therapeutic or other clinical purposes. An optimal choice of absorption coefficient (or wavelength), exposure duration, beam size, and radiant exposure to achieve a desired end-point can be derived from an analysis of model predictions. Such an optimal, or even an alternative choice may avoid undesirable but associated side effects. Collagen shrinkage occurs at up to 6 times the exposure level for minimum epithelial lesions for exposures less than 10^{-4} sec for absorption coefficients greater than 200 cm^{-1}. Hence, collagen shrinkage or other stromal effects may be avoided by using those exposure conditions (i.e., less than 10^{-4} sec with absorption coefficients greater than 200 cm^{-1}).

Currently thermokeratoplasty (TKP) is done with a small (3 mm diameter) TKP probe, heated to 90°C or 130°C and gently applied to the corneal surface for about 1 second (29, 61). However, undesired heating of

tissue surrounding the stroma complicates the desired therapeutic effects (24). It appears that this clinical technique could be enhanced by the use of an IR laser beam probe to heat the stroma, either by direct absorption or via conduction from the surface absorption at the epithelium. The procedure could be done in a few microseconds with a beam distribution designed for the shape of the keratoconus. Likewise, corneal (or lenticular) temperatures and their thermal effects can be predicted for exposure to ultraviolet wavelengths for threshold determinations; or even for exposure to the visible wavelengths for diagnostic techniques such as Raman spectroscopy, etc. Although water absorption becomes insignificant for the visible and ultraviolet wavelengths, corneal absorption coefficients remain about 1 cm^{-1} (up to $\simeq$ 100 cm^{-1}). A systematic analysis of a desired end-point and parameters available for thermal corneal effects can yield an optimal choice of parameter values much more effectively than the empirical approach.

CONCLUSIONS AND RECOMMENDATIONS

Available experimental damage threshold exposure data for IR lasers posing corneal hazards were analyzed for three damage end-points (minimal epithelial lesions, stromal collagen shrinkage or opacities, and epithelial vaporization or perforation). These damage thresholds were compared with thermal model predictions via several damage criteria for the specific experimental exposure conditions. This comparison provided a basis for credence in the thermal model predictions and justified its use to predict damage thresholds over the entire range of potential exposure conditions. When all three damage end-points are considered, the various threshold estimates are within a factor of between 3 and 10 of the mean experimental value. However, the damage integral predictions for the minimum epithelial lesion at the mean relative lesion radius were on the average 1.03 of the experimental value, and 90% of these predictions were within a factor of 2 of the experimental values.

In general terms, the thresholds for various damage end-points and criteria are proportional to critical peak temperature. The thresholds are inversely proportional to the absorption coefficient at lower values, but are independent of them for $\alpha \gtrsim 1000$ cm^{-1}. For beam radii greater than about 10^{-2} cm, thresholds are independent of beam radii. Thresholds are independent of the exposure duration for exposures less than about 10^{-4} sec. They are directly proportional to the exposure duration for exposures greater than about 1 second.

ANSI standards for the 1.4 - 1000 μm wavelength range appear to be adequate with the following reservations. Safety margins are excessive for absorption coefficients less than 200 cm^{-1} for exposures of less than about 10^{-2} sec. Safety margins for exposures longer than about 10^{-4} sec may be inadequate due to the large variation among threshold estimates and the permanent stromal effects that may result. Consideration of the wavelength (absorption coefficient), exposure duration, and damage end-point dependence of the threshold exposures developed in this study provides a basis for the continued development of IR safety criteria. These

more refined safety criteria will allow more realistic IR laser hazard evaluations.

Similar analyses with the thermal model--but for other applications, such as photokeratoplasty or corneal and lenticular spectroscopy--can yield alternative approaches to either maximize or avoid thermal effects often inherent in such research. Threshold estimates can be made for many exposure conditions from the data given in the tables and figures in this report.

We have obtained a much better agreement than expected between the thermal model and the experimental data, in spite of the many uncertainties and simplifications made for model input values. The agreement may have occurred because of excessive estimates of parameter variance, sensitivity, or a fortuitous balance of errors and sensitivities. This possibility is noted, not to decrease confidence in the model's usefulness, but to maintain a healthy skepticism and motivate research toward increasing the accuracy of the most significant model input parameter values.

Several alternative approaches and further avenues for research presented themselves during the study. The excellent results from the damage integral predictions at the mean lesion radius indicate its value as a damage criterion. This finding would give emphasis to experimental measurements of lesion radius to validate the model predictions. One might determine a similar or the same relationship for uniform beam distributions. Likewise, empirical CPT could be developed for the more permanent damage end-points. An empirical CPT for stromal damage would improve the accuracy of the model predictions. Empirical damage rates for the damage integral calculations for stromal effects could also be developed. Also, alternative choices of the depth of the damage site (i.e., not on the media layer boundaries) are suggested, possibly at depths in the midst of the tear or stromal layers. Although these alternate depths would not yield the lowest threshold estimate desired for the safety considerations, they may be more appropriate for other applications.

REFERENCES

1. AFM 161-32. Laser health hazards control. Washington D.C., 20 Apr 1973.

2. American national standard for the safe use of lasers. ANSI Z136.1-1976, New York, N.Y., 1976.

3. Anderson, F. A. Biological bases for and other aspects of a performance standard for laser products. DHEW No. (FDA) 75-8004, Bureau of Radiological Health, Rockville, Md., July 1974.

4. AR 40-46. Control of health hazards from lasers and other high intensity optical sources. Washington, D.C., 6 Feb 1974.

5. Army Technical Bulletin, TBMED 279. Control of hazards to health from laser radiation. Washington, D.C., 30 May 1975.

6. Boettner, E. A., and D. Dankovic. Ocular absorption of laser radiation for calculating personnel hazards, determination of the absorption coefficient in the ultraviolet and infrared of the ocular media of the rhesus monkey. Final report Contract F41609-74-C-0008, University of Michigan, Ann Arbor, Mich., Nov 1974. AD-A009176.

7. Borland, R. G., et al. Threshold levels for damage of the cornea following irradiation by a continuous wave-carbon dioxide (10.6 μm) laser. Nature 234:151-152 (1971).

8. Bowman, H. F., et al. Theory, measurement and application of thermal properties of biomaterials, pp. 48-80. In L. J. Mullins, et al. (eds.). Annual Review of Biophysics and Bioengineering, vol. 4. Palo Alto, Calif: Annual Review Inc., 1975.

9. Brownell, S., and B. E. Stuck. Ocular and skin hazards from CO_2 laser radiation. Army Science Conference Proceedings, vol. 1, pp. 123-138, 18-21 June 1974. AD-785609.

10. Byer, H. H., et al. Determination of the threshold of CO_2 laser corneal damage to owl monkeys, rhesus monkeys, and dutch belted rabbits. Memorandum Report M72-3-1, Joint AMRDC-AMC-Laser Safety Team, Feb 1972. AD-901086.

11. Campbell, C., Jr., et al. Ocular effects produced by experimental lasers: II. Carbon dioxide laser. Am J Ophthal 66(4):604-614 (1968).

12. Centano, M. V. The refractive index of liquid water in the near infrared spectrum. J Opt Soc Am 31:244-247 (1941).

13. Chang, H. H., and K. G. Dedrick. On corneal damage thresholds for CO_2 laser radiation. Appl Opt 8(4):826-827 (1969).

14. Clarke, A. M. Ocular hazards from lasers and other optical sources. CRC Critical Reviews in Environmental Control 1:307-339 (1970).

15. Coogan, P. S., et al. Histological and spectrophotometric comparison of the human and the rhesus monkey retina and pigmented ocular fundus. Final report Contract F41609-71-C-0006, Rush-Presbyterian St. Luke's Medical Center, Chicago, Ill., Jan 1974.

16. Curcio, J. A., and C. C. Petty. The near infrared absorption spectrum of liquid water. J Opt Soc Am 41:302-304 (1951).

17. Downing, H. D., and D. Williams. Optical constants of water in the infrared. J Geophy Res 80(12):1656-1661 (Apr 1975).

18. Dunsky, I. L., and D. E. Egbert. Corneal damage thresholds for hydrogen fluoride and deuterium fluoride chemical lasers. SAM-TR-73-51, Dec 1973.

19. Dunsky, I. L., et al. Determination of revised Air Force permissible exposure levels for laser radiation. Am Indust Hyg Assoc J 34(6) 235-240 (1973).

20. Fine, B. S., et al. CO_2 laser irradiation of the rabbit eye, clinical and histopathological observations. IEEE Cat. No. 70, NEREM 8:160-161, 1966.

21. Fine, B. S., et al. Preliminary observations of ocular effects of high-power continuous CO_2 laser irradiation. Am J Ophthalmol 64(2):209-222 (1967).

22. Fine, B. S. Corneal injury threshold to carbon dioxide laser irradiation. Am J Ophthalmol 66(1):1-15 (1968).

23. Fine, S., et al. Biophysical studies with the CO_2 laser. IEEE Cat. No. 70 NEREM 8:166-167, 1966.

24. Fogle, J. A., et al. Damage to epithelial basement membrane by thermokeratoplasty. Am J Ophthalmol 83(3):392-401 (1977).

25. Freeman, R. D., and I. Fatt. Environmental influences on ocular temperature. Invest Ophthalmol 12(8):596-602 (1973).

26. Fugitt, C. H. A rate process theory of thermal injury. AF Special Weapons Project Report No. 606, 6 Dec 1955. AD-212660.

27. Gallagher, J. T. Corneal curvature changes due to exposures to a carbon dioxide laser: A preliminary report. SAM-TR-75-44, Dec 1975.

28. Garrett, R. R., and P. J. Flory. Evidence for a reversible first order phase transition in collagen-diluent mixtures. Nature 177:176-177 (1956).

29. Gasset, A. R., et al. Thermokeratoplasty. Trans Am Acad Ophthalmol Otolaryngol 77:OP-442-454 (1973).

30. Geeraets, W., et al. Ocular injury from CO_2 laser irradiation. Acta Ophthalmol 47:80-92 (1969).

31. Gullberg, K., et al. Carbon dioxide laser hazards to the eye. Nature 215:857-858 (1967).

32. Gustavson, K. H. The chemistry and reactivity of collagen, pp. 211-227, New York: Academic Press, 1956.

33. Hale, G., and M. R. Querry. Optical constants of water in the 200 nm to 200 μm wavelength region. Appl Opt 12(3):555-563 (1973).

34. Heimbach, C. R. Models of heat dissipation in a homogeneous solid. USAMRL Report No. 954. 1971, AD-738789.

35. Henriques, F. C. Studies of thermal injury. V. The predictability and the significance of thermally induced rate processes leading to irreversible epidermal injury. Arch Pathol 43(5):489-502 (1974).

36. Henriques, F. C., and A. R. Meritz. Studies of thermal injury. I. The conduction of heat to and through skin and the temperature attained therein, a theoretical and experimental investigation. Am J Pathol 23(4):531-550 (1947).

37. Irvine, W. M., and J. B. Pollack. Infrared optical properties of water and ice spheres. Icarus 8:324-360 (1968).

38. Laser products performance standards. DHEW, FDA (BRH) Federal Register 40(148):32251-32266 (1975).

39. Leibowitz, H. H., and G. R. Peacock. Corneal injury produced by CO_2 laser radiation. USAMRL Report No. 787 (1968).

40. Leibowitz, H. H., and G. R. Peacock. Corneal injury produced by carbon dioxide laser radiation. Arch Ophthalmol 81:713-721 (1969).

41. Lund, D. J., et al. Ocular hazards of the Q-switched erbium laser. Invest Ophthalmol 9(6):463-470 (1970).

42. MacKeen, D., et al. Simultaneous corneal surface and anterior chamber temperature measurements on CO_2 laser irradiation. (Abstract) Fed Proc 33(3), part 1:461 (1974).

43. Mainster, M. A., et al. Corneal thermal response to the CO_2 laser. Appl Opt 9(3):665-667 (1970).

44. Mapstone, R. Normal thermal patterns in cornea and periorbital skin. Brit J Ophthalmol 52:818-827 (1968).

45. Mikesell, G. W. Laser Effects Branch, USAF School of Aerospace Medicine, Brooks AFB, Tex. Personal communication, 30 July 1976.

46. Mishima, A., and D. M. Maurice. The effect of normal evaporation on the eye. Exp Eye Res 1:46-52 (1961).

47. Mishima, S. Some physiological aspects of the precorneal tear film. Arch Ophthalmol 73:233-241 (1965).

48. Moritz, A. R., and F. C. Henriques. Studies of thermal injury. II. The relative importance of time and surface temperature in the causation of cutaneous burns. Am J Pathol 23:695-720 (1947).

49. Mueller, H. A., and W. T. Ham. The ocular effects of single pulses of 10.6 μm and 2.5-30 μm Q-switched laser radiation--A report to the Los Alamos Scientific Lab L-Div. Virginia Commonwealth University, Richmond, Va., undated.

50. Palmer, K. F., and D. Williams. Optical properties of water in the near infrared. J Opt Soc Am 64(8):1107-1110 (1974).

51. Peabody, R., et al. Threshold damage from CO_2 la[illegible]s. Arch Ophthalmol 82:105-107 (1969).

52. Peacock, G. R. Surface temperature as a parameter in estimating laser injury thresholds. USAMRL Report No. 733, 8 June 1967.

53. Peacock, G. R. Near infrared lasers: Safety calculations. USAMRL Report No. 761, 26 Dec 1967.

54. Peppers, N., et al. Corneal damage thresholds for CO_2 laser radiation. Appl Opt 8(2):377-381 (1969).

55. Priebe, L. A., and A. J. Welch. The measurement of threshold temperatures in the ocular fundus for laser induced visible lesions. Technical Report No. 180, Electronics Res. Ctr., Univ. of Texas at Austin, 1 Feb 1976.

56. Prince, J. H. The rabbit in eye research, p. 98. Springfield, Ill.: Charles C Thomas, 1964.

57. Querry, M. R., et al. Refractive index of water in the infrared. J Opt Soc Am 59(10):1299-1305 (1969).

58. Robertson, C. W., and D. Williams. Lambert absorption coefficients of water in the infrared. J Opt Soc Am 61(10):1316-1320 (1971).

59. Rusk, A. N., et al. Optical constants of water in the infrared. J Opt Soc Am 61(7):895-903 (1971).

60. Schwartz, B., and M. R. Feller. Temperature gradients in the rabbit eye. Invest Ophthalmol 1:513-521 (1952).

61. Shaw, E. L., and A. R. Gasset. Thermokeratoplasty (TKP) temperature profile. Invest Ophthalmol 13(3):181-186 (1974).

62. Sliney, D. H. The development of laser safety criteria, pp. 163-238. In M. L. Wolbarsht (ed.). Laser applications in medicine and biology. New York: Plenum Press, 1971.

63. Sliney, D. H., and B. C. Freasier, Evaluation of optical radiation hazards. Appl Opt 12(1):1-24 (1973).

64. Spencer, D. J., and I. L. Dunsky. Preliminary corneal damage threshold studies with HF-DF chemical lasers. SAMSO-TR-73-215, 15 July 1973.

65. Stringer, H., and J. Parr. Shrinkage temperature of eye collagen. Nature 204:1307 (1964).

66. Stuck, B. E. Corneal damage thresholds for carbon dioxide laser irradiation. Presented at Third Meeting of TTCP J-10 Working Group A (Laser Hazards), Ottawa, Canada, June 1972.

67. Stuck, B. E. Letterman Army Institute of Research, Presidio, Calif. Personal communication, 24 Mar 1977.

68. Takata, A. N. Development of criterion for skin burns. Aerospace Med 45:634-637 (1974).

69. Takata, A. N., et al. Thermal model of laser-induced eye damage. Final report Contract F41609-74-C-0005, IIT Research Institute, Oct 1974. AD-A-917201.

70. Van Pelt, W. F., et al. A review of selected bioeffects thresholds for various ranges of light. DHEW Publication No. (FDA) 74-8010, Bureau of Radiological Health, Rockville, Md.,1973.

71. Vassiliadis, A., et al. Investigation of laser damage to ocular tissues. AFAL-TR-67-170, Contract AF33615-3060, Stanford Research Institute, Menlo Park, Calif, Mar 1967.

72. Vassiliadis, A., et al. Investigations of laser damage to ocular tissues. Final report Contract AF33615-67-C-1752, Stanford Research Institute, Menlo Park, Calif, Mar 1968.

73. Vassiliadis, A., et al. Thresholds of laser eye hazards. Arch Environ Health 20:161-170 (1970).

74. Vassiliadis, A., et al. Ocular damage from laser radiation, pp. 125-162. In M. L. Wolbarsht (ed.). Laser applications in medicine and biology. New York: Plenum Press, 1971.

75. Welch, A. J. Model of thermal injury based on temperature rise in fundus exposed to laser radiation. Final report Contract F41609-74-C-0025, University of Texas at Austin, Aug 1975.

76. Welch A. J., et al. Limits of applicability of thermal models of thermal injury. Final report Contract F41609-76-C-0005, University of Texas at Austin, Aug 1976.

77. Winburn, D. C. Safety considerations in the laser research program at the Los Alamos Scientific Laboratory. In L. Goldman (ed.). Third Conference on Lasers, New York Academy of Sciences (1975), vol. 267, 30 Jan 1976.

78. Winburn, D. C. Safety aspects of laser fusion research at the Los Alamos Scientific Laboratory. Optics and Technology 8(6):265-267 (1976).

79. Zolotarev, V. M., et al. Dispersion and absorption of liquid water in the infrared and radio regions of the spectrum. Opt Spectrosk 27: 790 (1969), Opt Spectrosc, English Trans, 27:430 (1969).

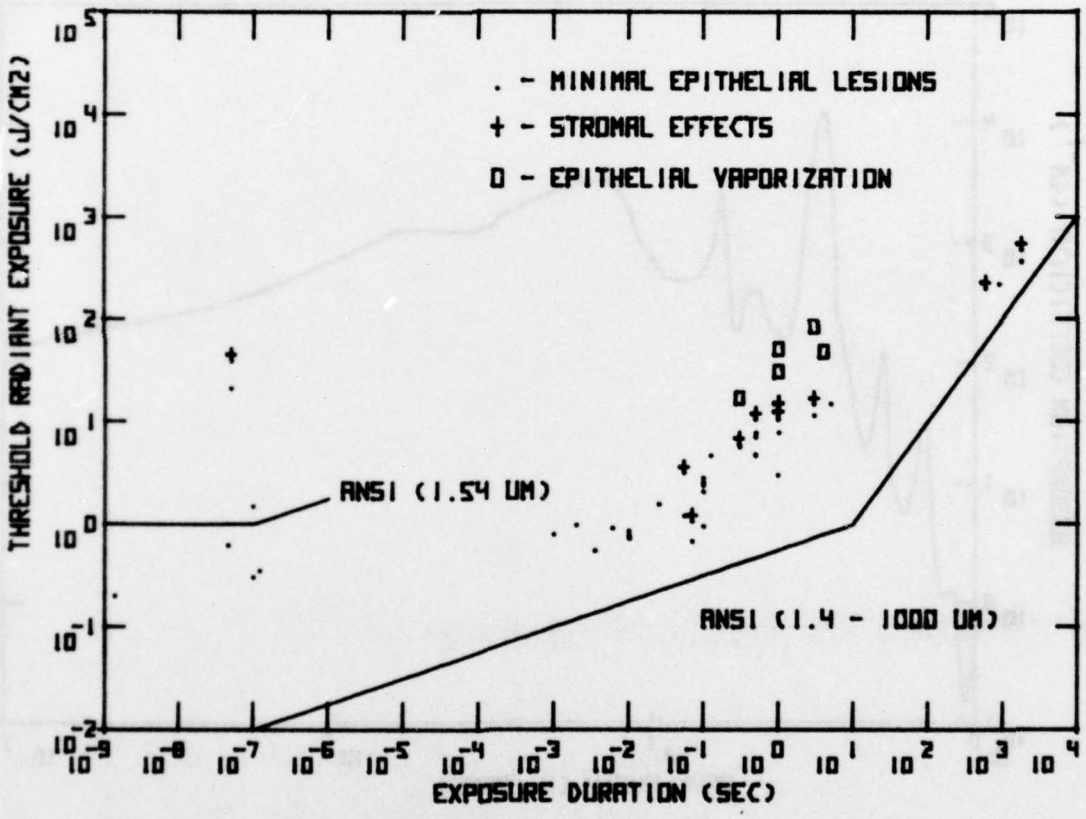

Figure 1. Experimental corneal thresholds and ANSI standards vs. exposure duration: minimum epithelial lesion, stromal effects, and epithelial vaporization thresholds (see Tables 1 - 3).

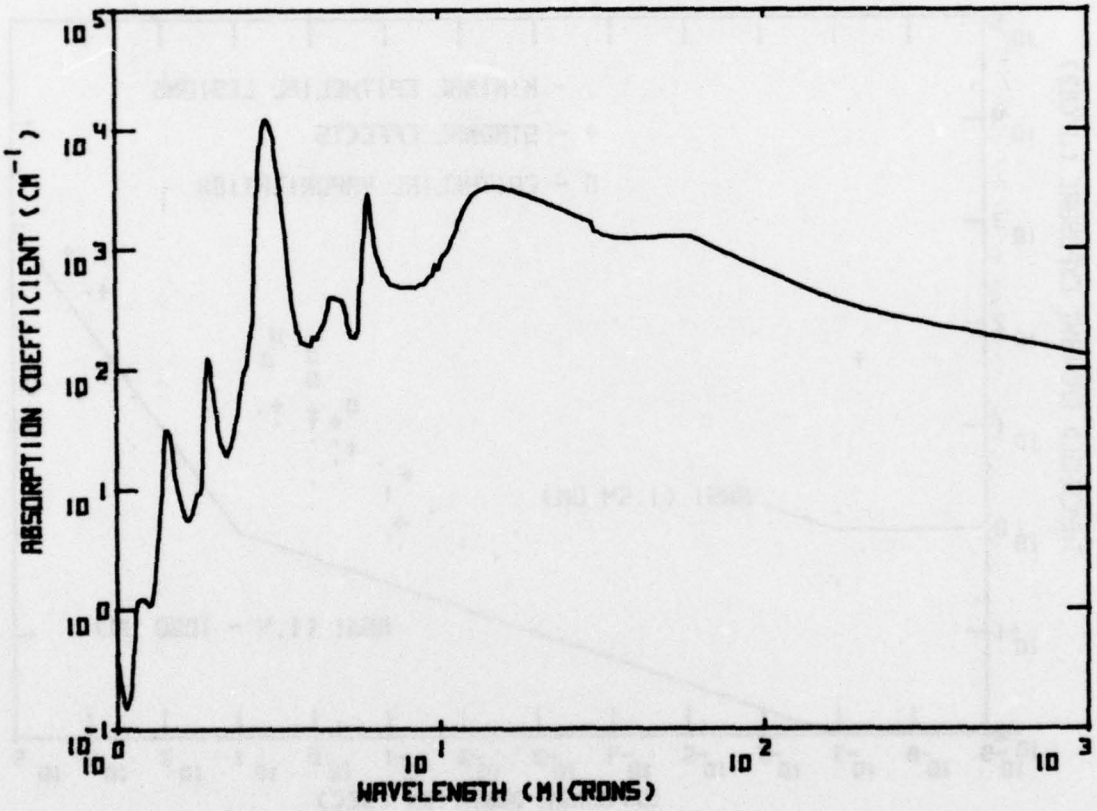

Figure 2. Water absorption spectrum (50, 59, 79).

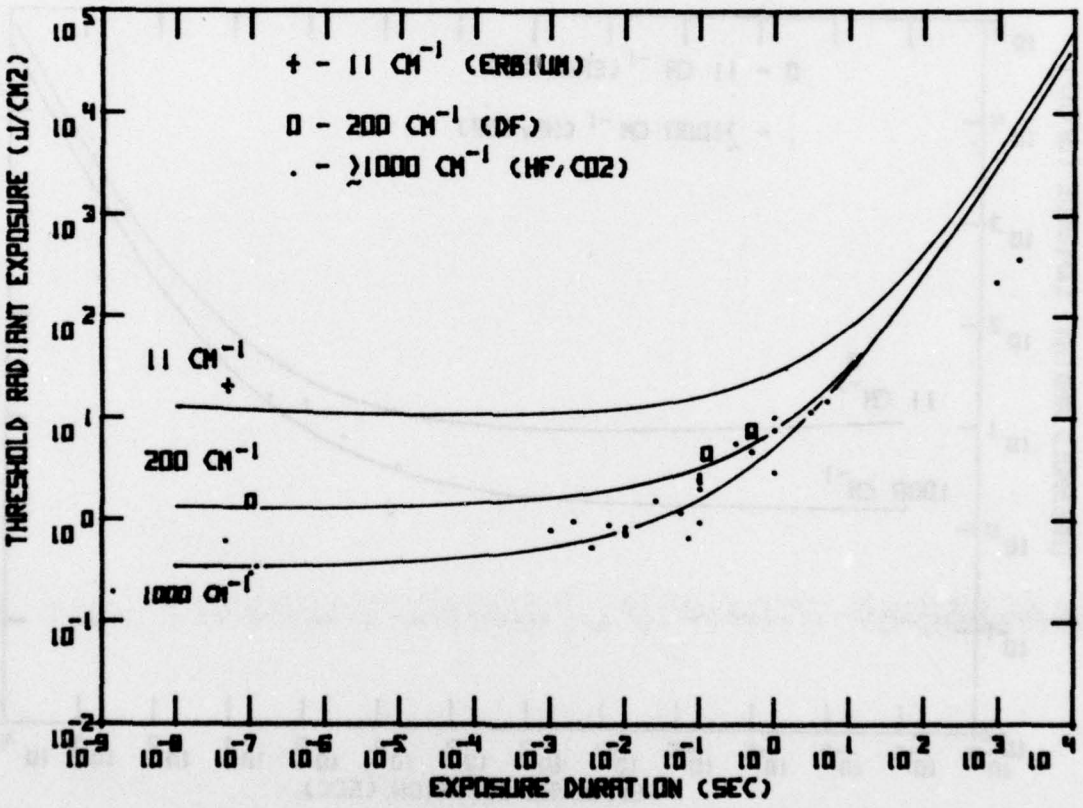

Figure 3. Comparison of experimental and theoretical epithelial lesion thresholds for absorption coefficients equal to 11 cm^{-1}, 200 cm^{-1}, and 1000 cm^{-1}.

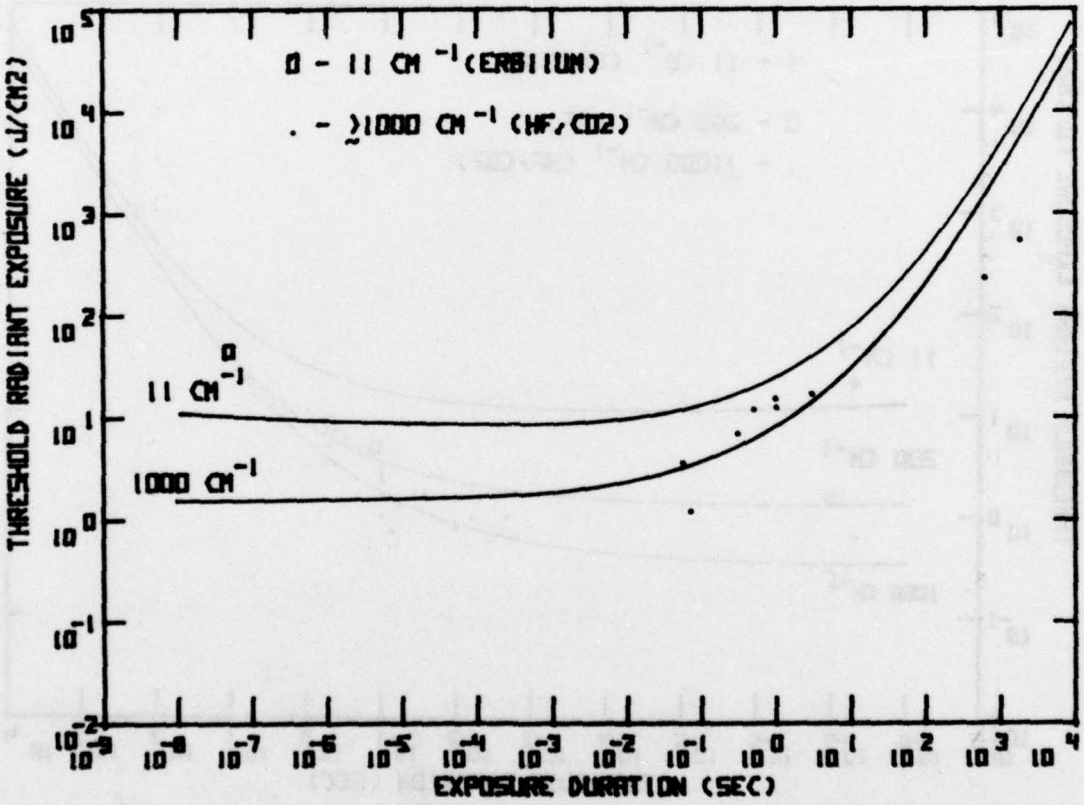

Figure 4. Comparison of experimental and theoretical stromal thresholds for absorption coefficients equal to 11 cm^{-1} and 1000 cm^{-1}.

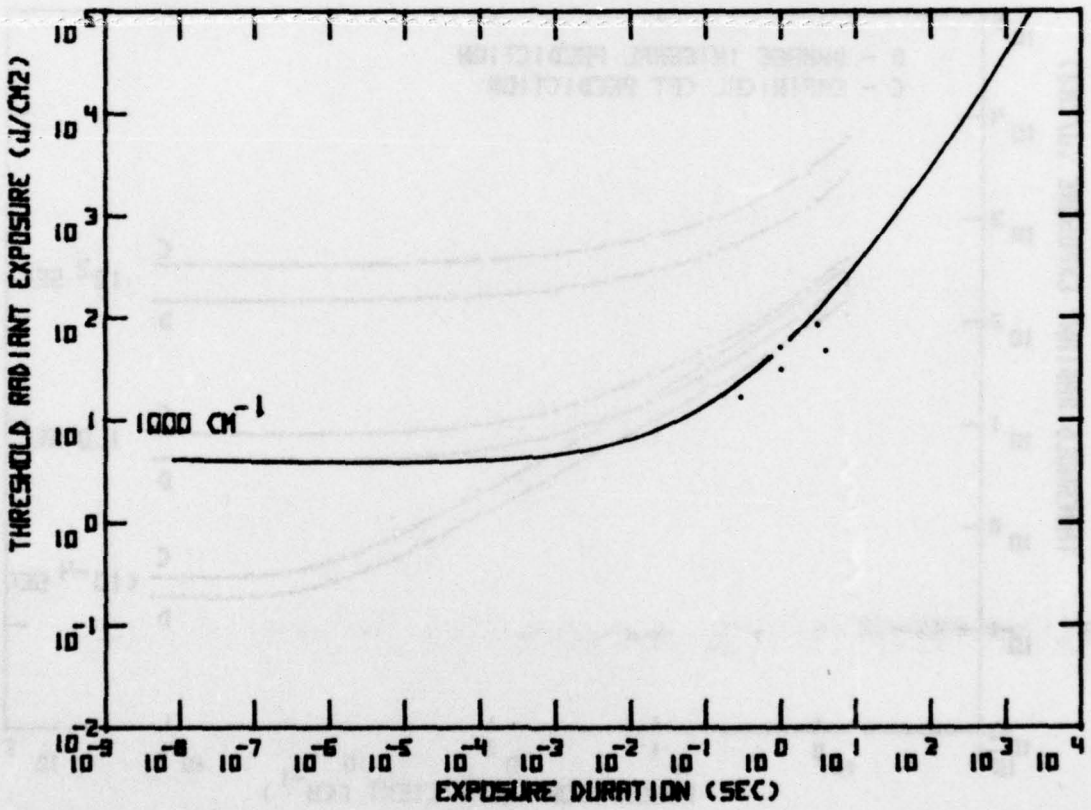

Figure 5. Comparison of experimental and theoretical epithelial vaporization for an absorption coefficient equal to 1000 cm^{-1}.

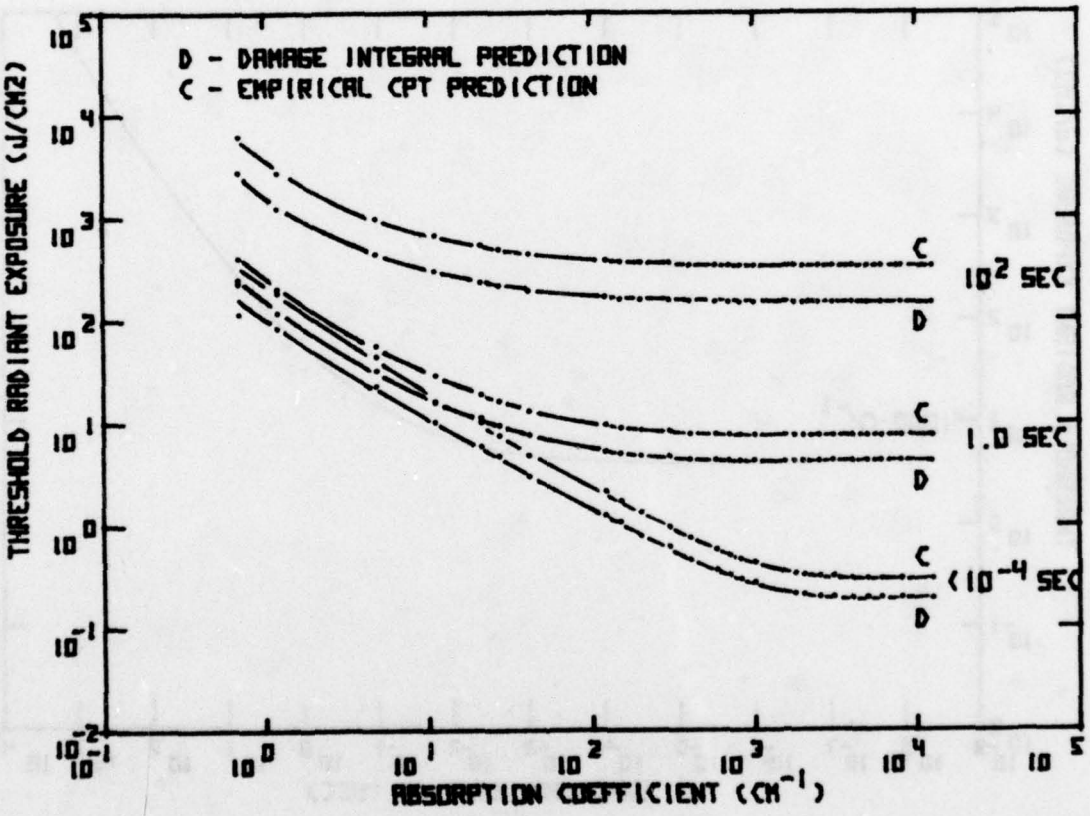

Figure 6. Epithelial lesion threshold vs. absorption coefficient for 0.07 cm beam radius (1/e) for $\leq 10^{-4}$, 1.0, and 10^{2} sec exposures.

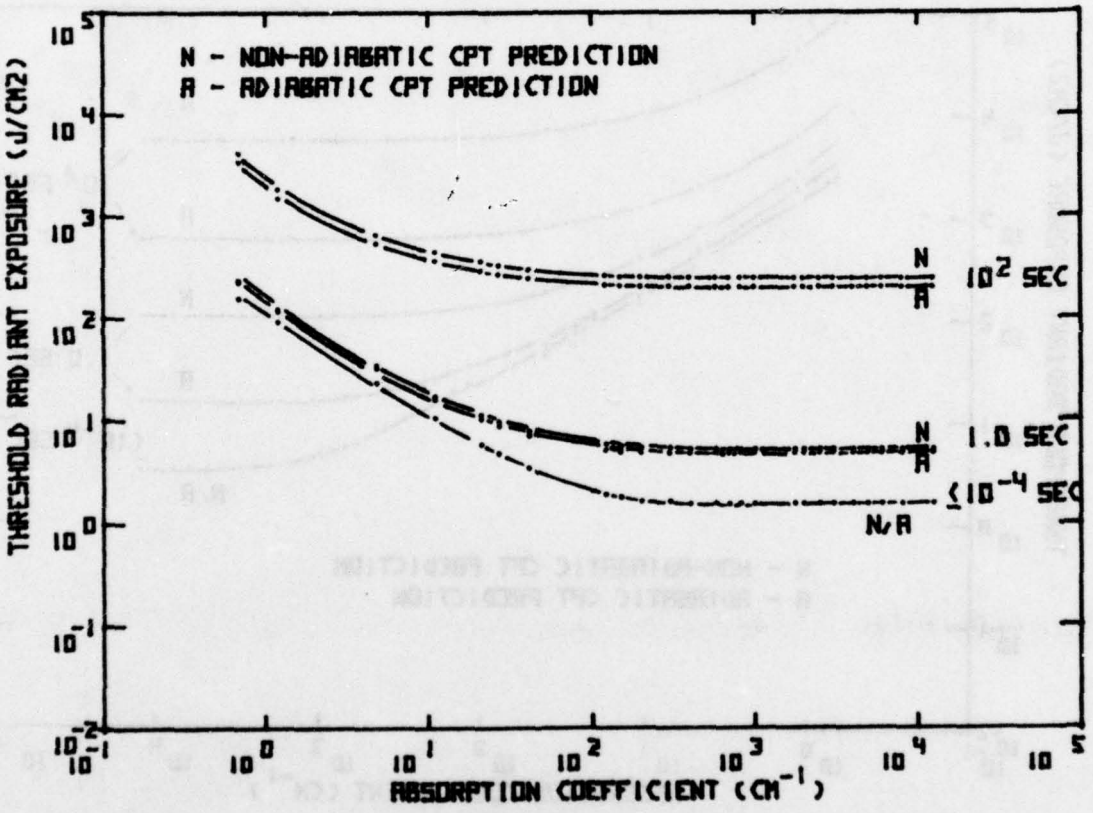

Figure 7. Stromal collagen shrinkage threshold vs. absorption coefficient for 0.07 cm beam radius (1/e) for $\leq 10^{-4}$, 1.0, and 10^2 sec exposures.

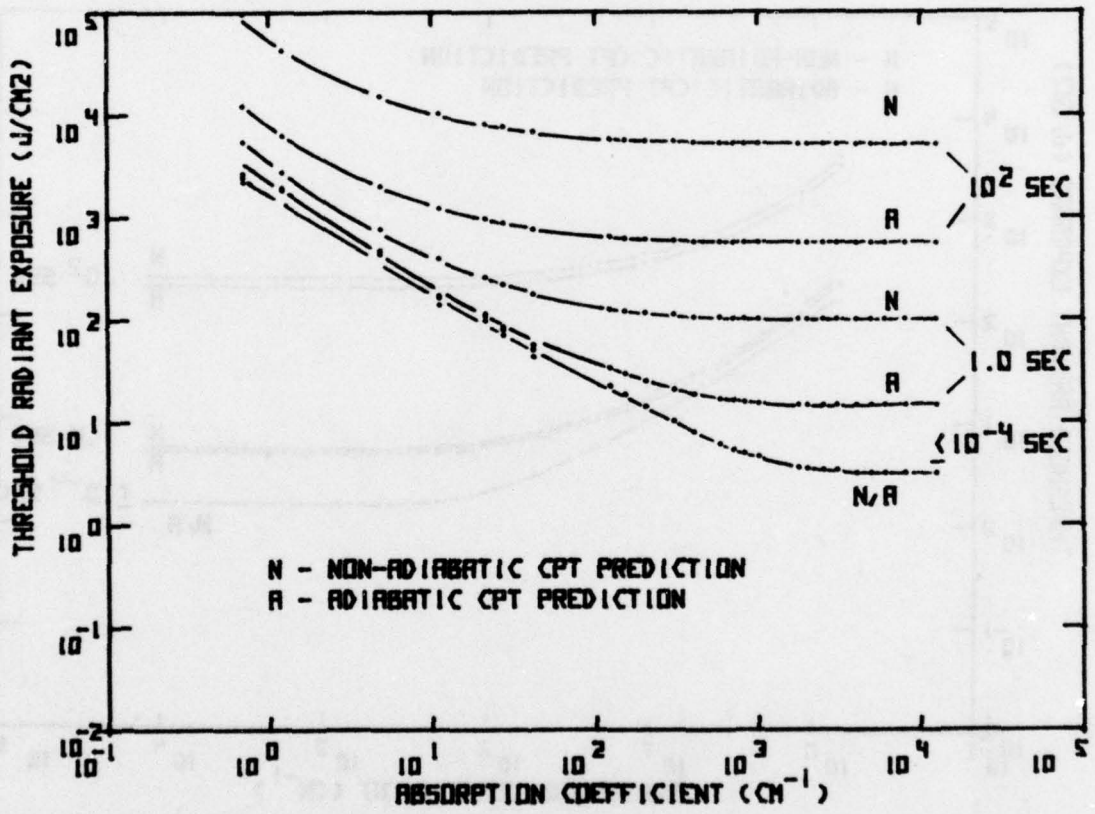

Figure 8. Epithelial vaporization threshold vs. absorption coefficient for 0.07 cm beam radius (1/e) for $\leq 10^{-4}$, 1.0, and 10^2 sec exposures.

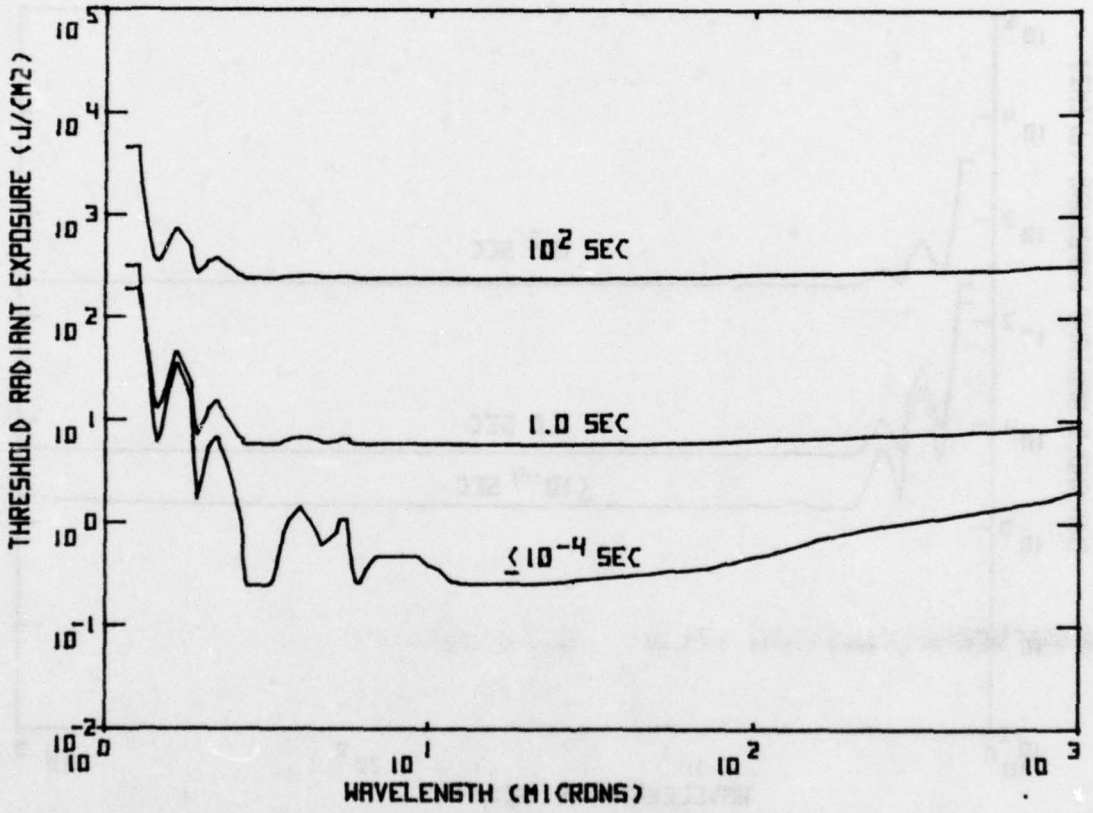

Figure 9. Epithelial lesion threshold vs. wavelength for 0.07 cm beam radius (1/e) for $\leq 10^{-4}$, 1.0, and 10^2 sec exposures.

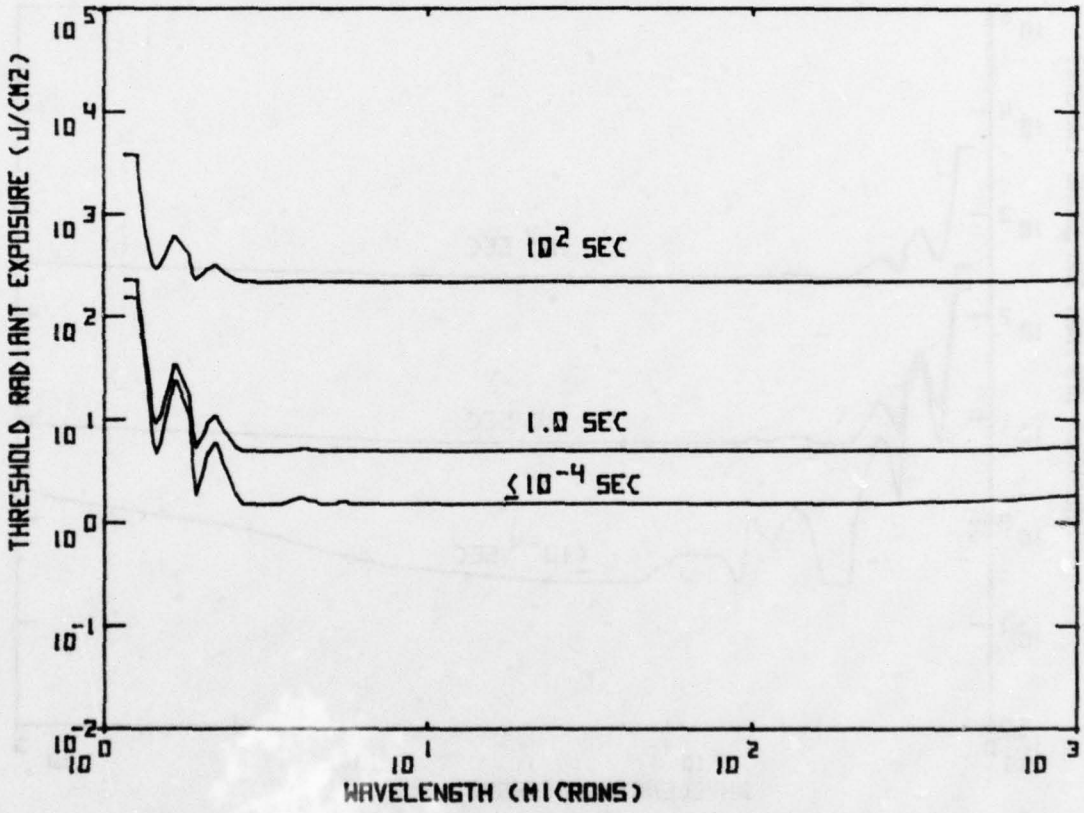

Figure 10. Stromal collagen shrinkage threshold vs. wavelength for 0.07 cm beam radius (1/e) for $\leq 10^{-4}$, 1.0, and 10^2 sec exposures.

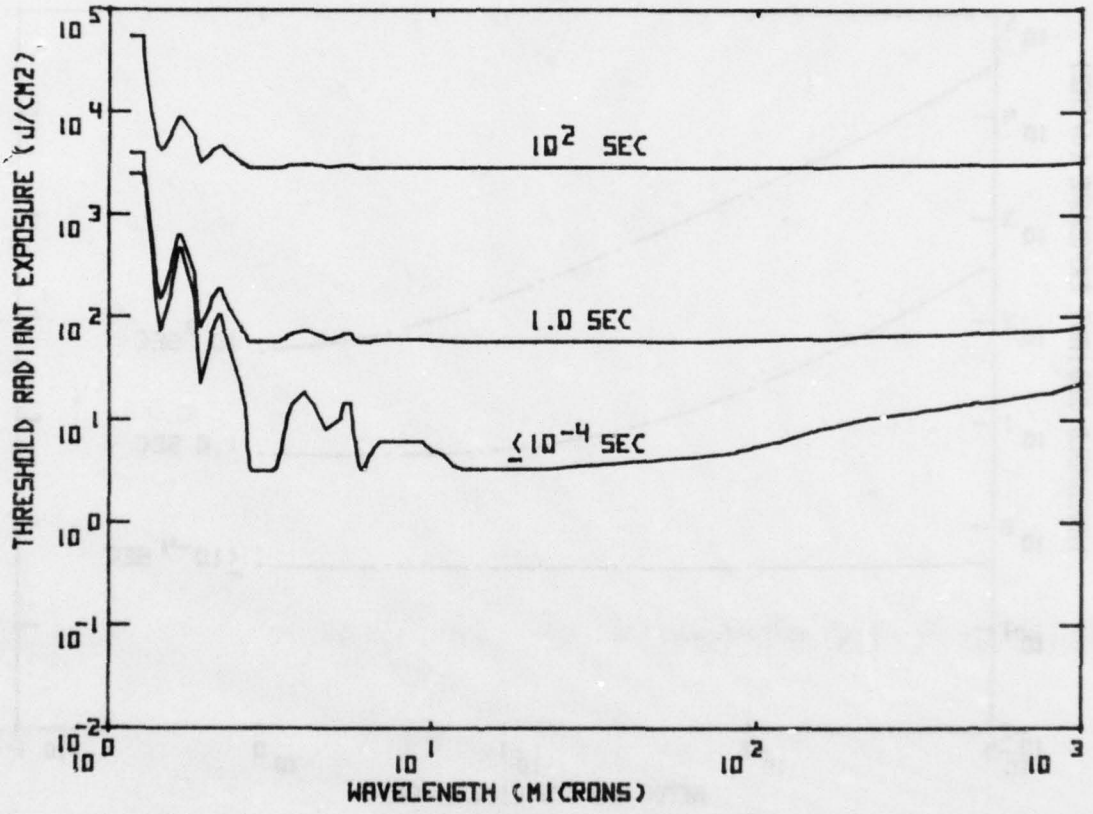

Figure 11. Epithelial vaporization threshold vs. wavelength for 0.07 cm beam radius (1/e) for $\leq 10^{-4}$, 1.0, and 10^2 sec exposures.

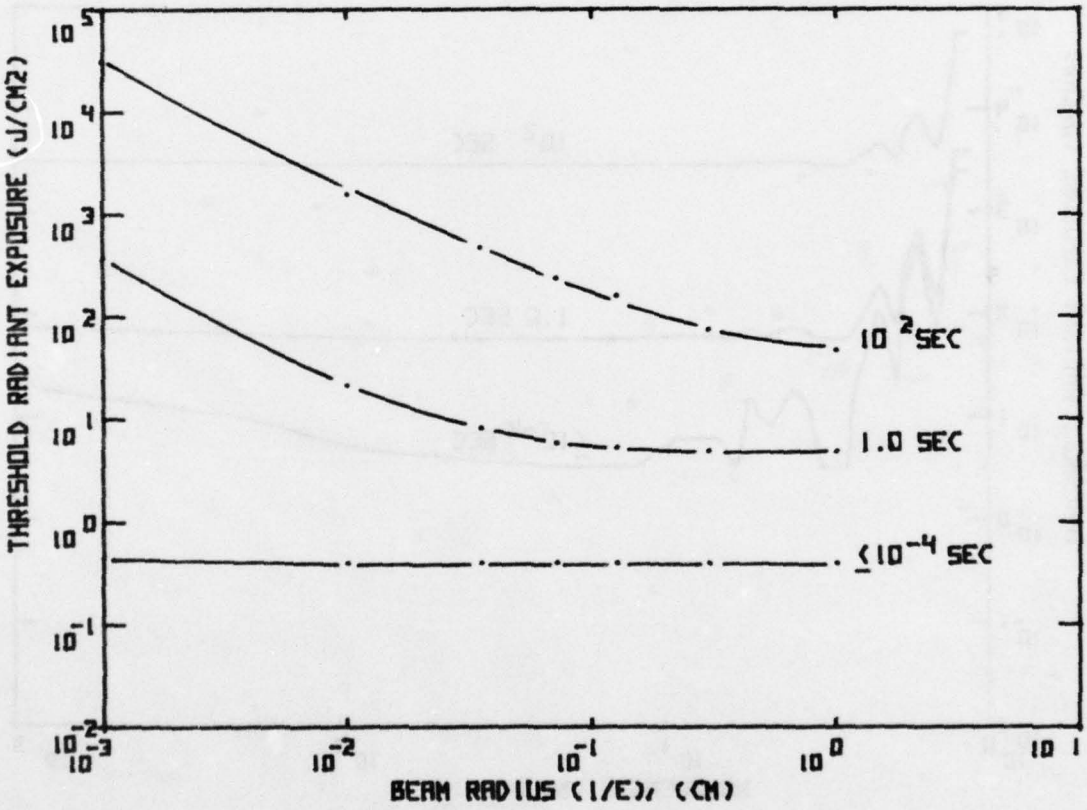

Figure 12. Epithelial lesion threshold vs. beam radius for $\leq 10^{-4}$, 1.0, and 10^{2} sec exposures at an absorption coefficient of 817 cm^{-1}.

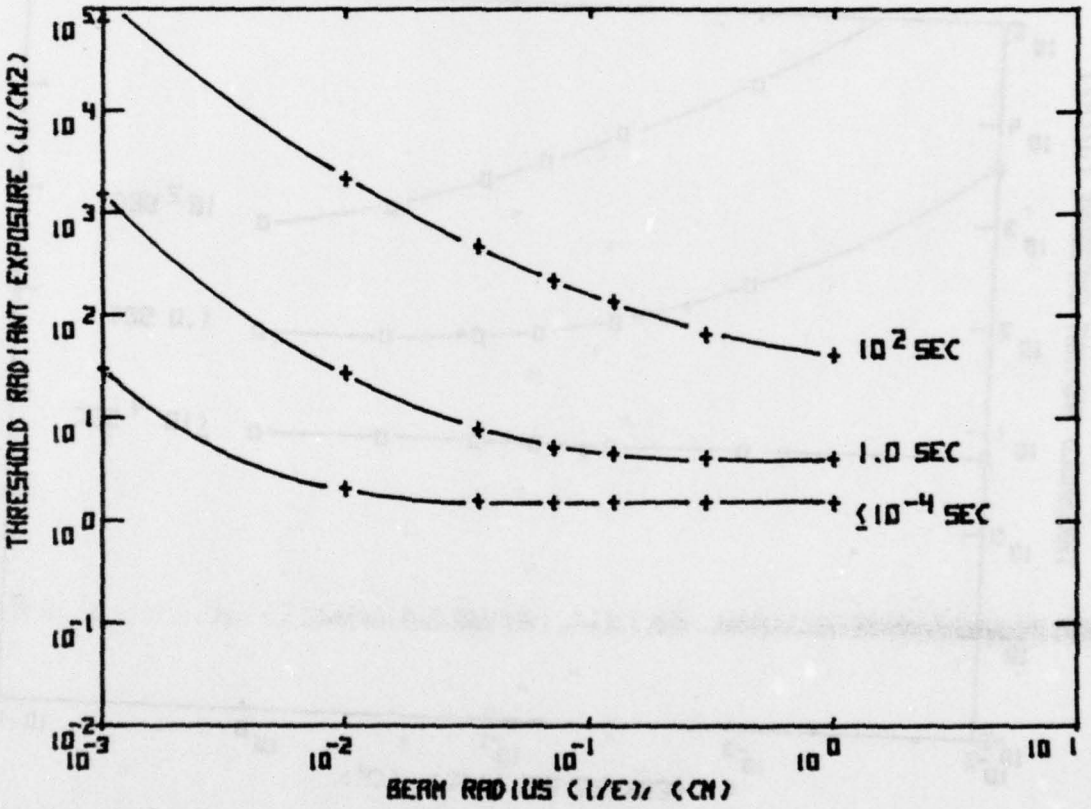

Figure 13. Stromal collagen shrinkage thresholds vs. beam radius for $\leq 10^{-4}$, 1.0, and 10^2 sec exposures at an absorption coefficient of 817 cm^{-1}.

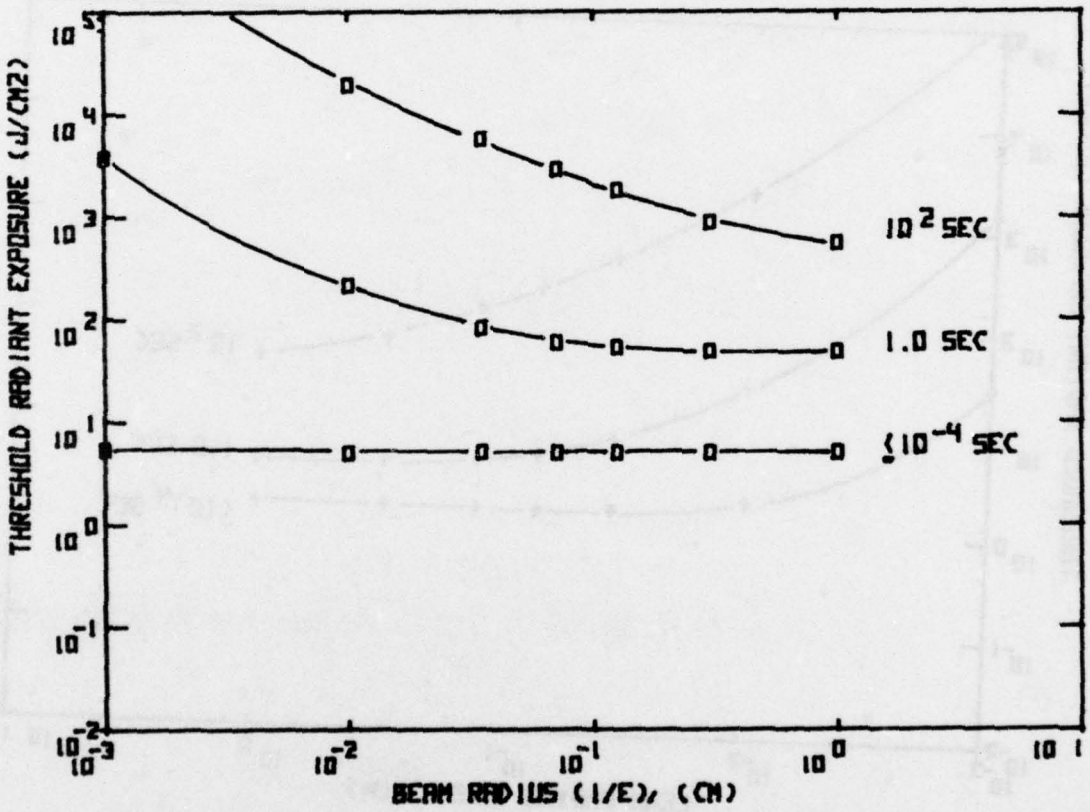

Figure 14. Epithelial vaporization thresholds vs. beam radius for $\leq 10^{-4}$, 1.0, and 10^{2} sec exposures at an absorption coefficient of 817 cm^{-1}.

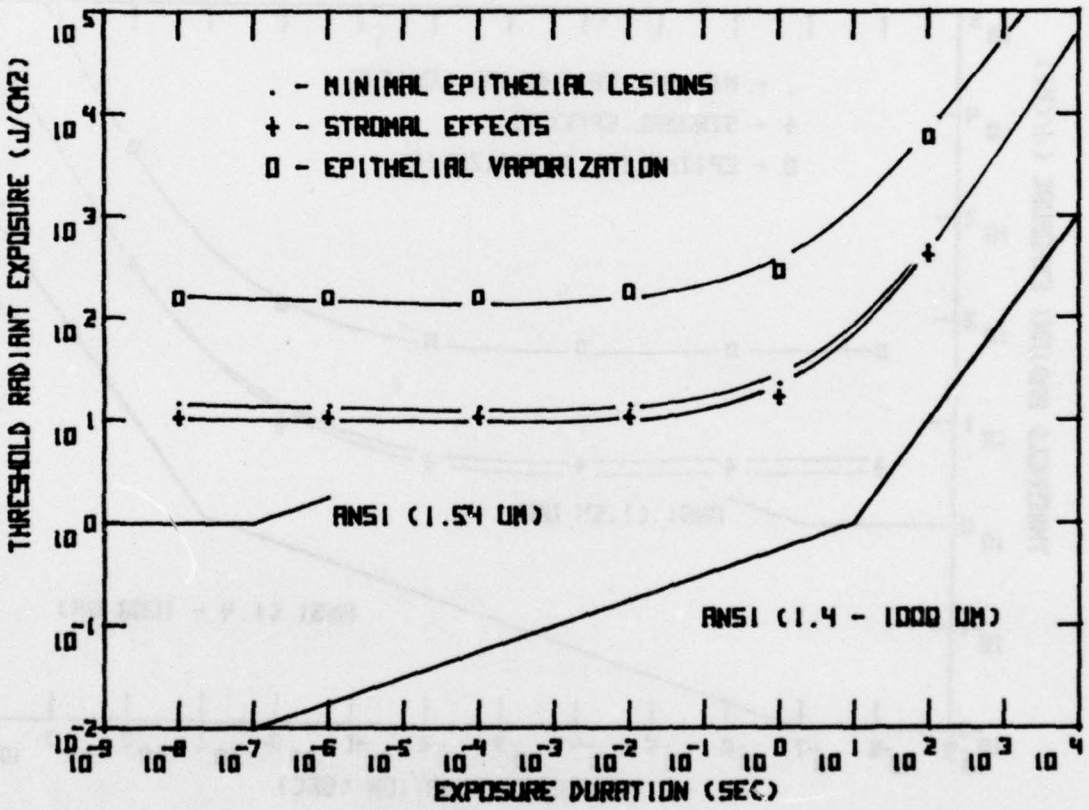

Figure 15. Damage thresholds for erbium lasers (1.54 μm, ≈11 cm^{-1}) vs. exposure duration.

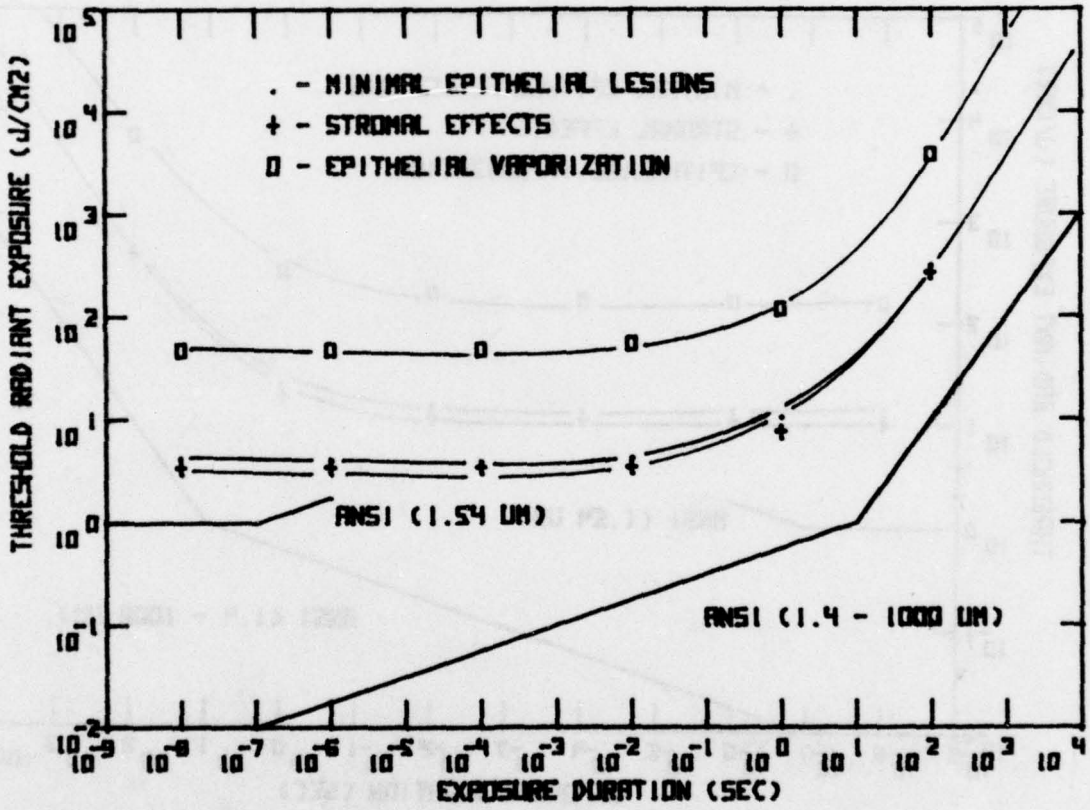

Figure 16. Damage thresholds for holmium lasers (2.06 μm, ≈41 cm^{-1}) vs. exposure duration.

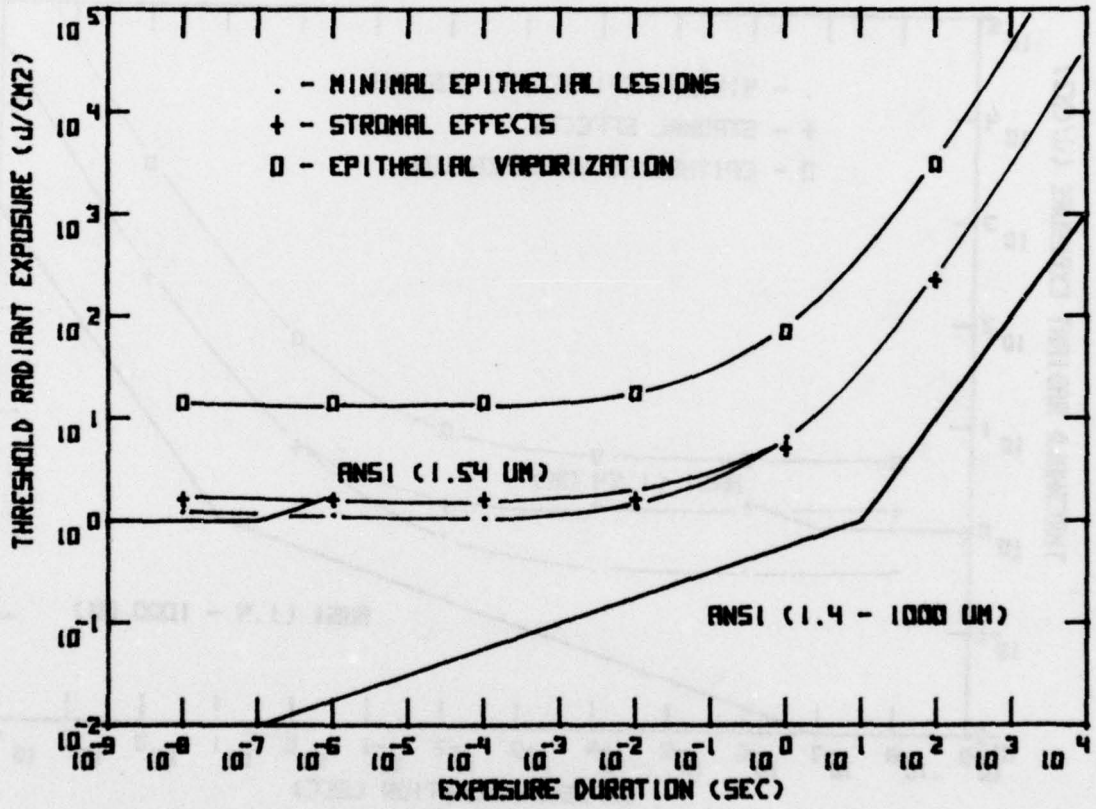

Figure 17. Damage thresholds for DF and CO (3.5 - 5.0 μm, ≈200 cm^{-1}) vs. exposure duration.

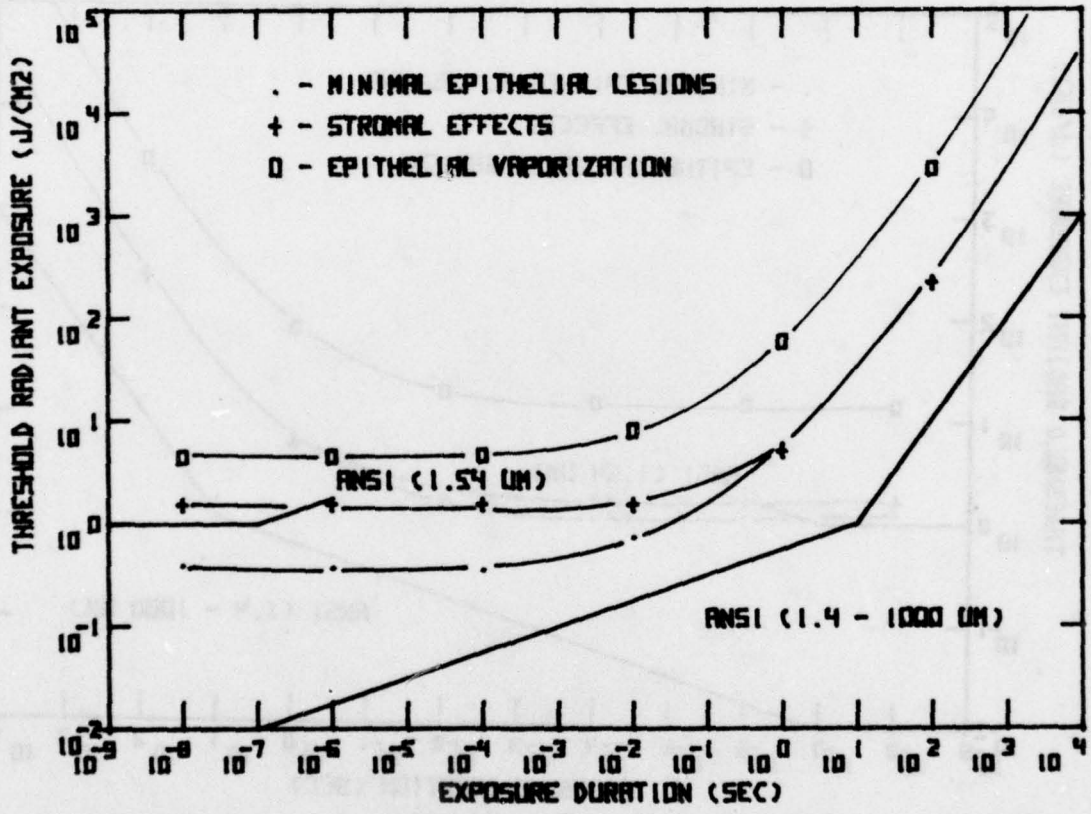

Figure 18. Damage thresholds for HF and CO_2 (2.5 - 3.0 and 10.6 μm, ≥1000 cm^{-1}) vs. exposure duration.

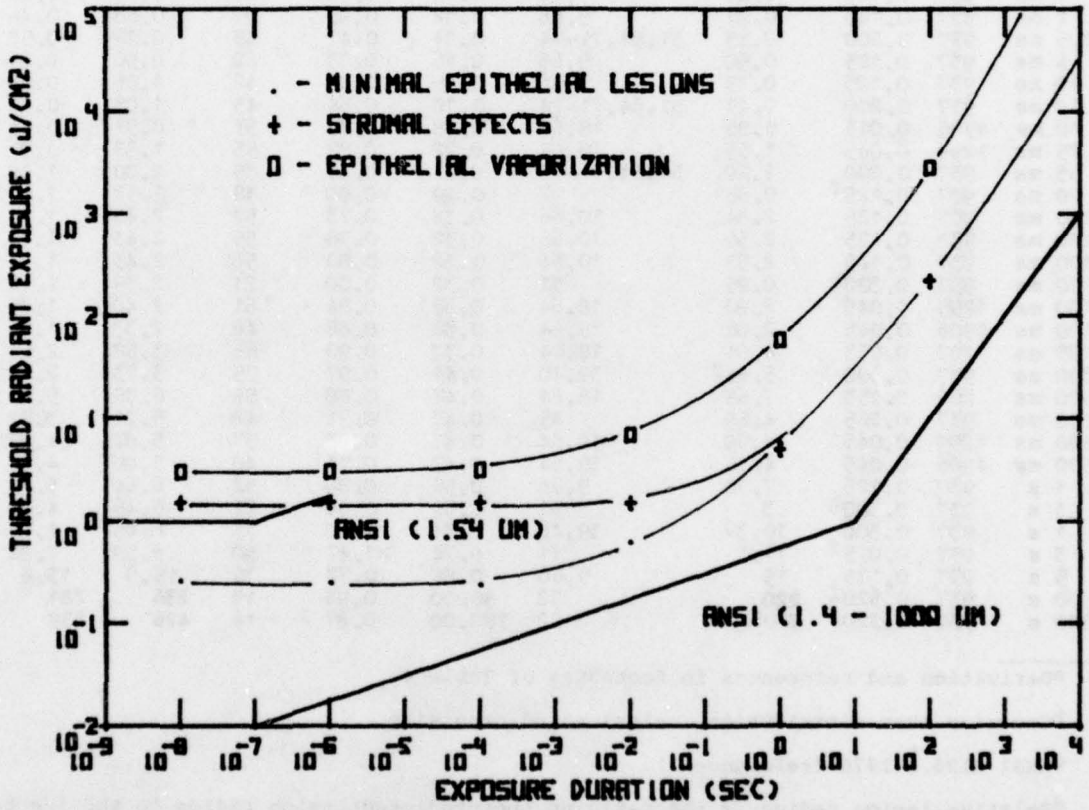

Figure 19. Damage thresholds for HF (2.94 μm, 12395 cm^{-1}) vs. exposure duration.

TABLE 1. MINIMUM CORNEAL EPITHELIAL LESIONS FROM IR LASER EXPOSURE: EXPERIMENTAL EXPOSURE CONDITIONS, MODEL PREDICTIONS, AND ANSI STANDARDS. MODEL PREDICTIONS ARE MADE FOR A DEPTH OF 6 μm

Experimental Exposure Conditions					ANSI	Model Predictions			
					Laser expos. stand.[c]	For experiment threshold, $H_{\ell e}$		Predicted thresholds[e]	
Exposure duration	Absorp. coeff.[a] (cm^{-1})	Beam radius[b] r(1/e) (cm)	Exper. thresh. $H_{\ell e}$ (J/cm^2)	Experimental references	H_{ANSI} (J/cm^2)	Relative lesion[d] radius	Temp. rise (°C)	$H_{\ell di}$ at $r=r_\ell$ (J/cm^2)	$H_{\ell a}$ at r=0 (J/cm^2)
1.4 ns	937	0.475[f]	0.2[g]	49,77,78	0.01	0.00	32	0.27	0.41
45 ns	3220	0.020	0.62	18,64	0.01	1.10	126	0.33	0.27
50 ns	12	0.028	21	41	1.00	0.88	61	17.30	16.60
100 ns	197	0.024[h]	1.51	18,64	0.01	0.76	62	1.51	1.24
100 ns	11190	0.300[h]	0.3[g]	49,77,78	0.01	0.68	59	0.34	0.26
120 ns	937	0.160	0.35	67	0.01	0.48	47	0.52	0.38
1 ms	937	0.125	0.80	9,66	0.10	0.94	86	0.59	0.41
2 ms	937	0.125	0.97	9,66	0.12	0.95	91	0.68	0.46
3.5 ms	937	0.200	0.55	51,54,71-74	0.14	0.47	45	0.77	0.53
6 ms	937	0.125	0.90	9,66	0.16	0.73	62	0.96	0.61
10 ms	937	0.125	0.73	9,66	0.18	0.48	42	1.06	0.72
10 ms	937	0.200	0.77	51,54,71-74	0.18	0.54	45	1.08	0.72
10 ms	4906	0.045	0.86	18,64	0.18	0.74	57	0.91	0.63
25 ms	1299	0.045	1.55	18,64	0.22	0.82	65	1.38	0.97
55 ms	937	0.200	1.20	51,54,71-74	0.27	0.35	35	2.00	1.36
70 ms	937	0.125[f]	0.68[i]	7	0.29	0.00	18	1.12	1.47
100 ms	937	0.125	2.34	10,66	0.32	0.73	52	2.43	1.74
100 ms	937	0.125	2.50	10,66	0.32	0.78	55	2.43	1.74
100 ms	937	0.125	2.57	10,66	0.32	0.80	56	2.43	1.74
100 ms	937	0.300[h]	0.95	31	0.32	0.00	21	2.39	1.72
100 ms	1299	0.045	2.80	18,64	0.32	0.84	61	2.40	1.79
100 ms	4906	0.045	2.06	18,64	0.32	0.68	46	2.33	1.75
125 ms	202	0.053	4.61	18,64	0.33	0.90	66	3.58	2.62
300 ms	937	0.300	5.64[j]	39,40	0.41	0.97	75	3.73	2.75
500 ms	202	0.053	7.68	18,64	0.47	0.88	55	6.36	5.00
500 ms	937	0.265	4.69	45	0.47	0.71	48	5.21	3.52
500 ms	1299	0.045	6.99	18,64	0.47	0.93	57	5.07	4.37
500 ms	4906	0.045	4.76	18,64	0.47	0.74	40	5.00	4.32
1 s	937	0.125	7.70	9,66	0.56	0.88	52	6.64	5.20
1 s	937	0.300[h]	3	31	0.56	0.00	22	6.46	4.80
1 s	937	0.300	10.3[j]	39,40	0.56	1.00	75	6.46	4.82
3 s	937	0.075[f]	11.6	11	0.74	>1.47	50	5.58	7.82
5 s	937	0.125	15	9,66	0.84	0.72	36	15.9	13.6
900 s	937	0.520[f]	220	22	90.00	0.93	19	236	281
1800 s	937	0.520[f]	360[g]	22	180.00	0.87	16	426	539

[a] Derivation and references in footnotes of Table 4.

[b] Gaussian beam distribution, unless noted otherwise.

[c] ANSI Z136.1-1976 (reference 2).

[d] Relative lesion radius is the ratio of the predicted lesion radius to the 1/e beam radiu

[e] $H_{\ell a}$ is the average of the threshold dose predicted via the damage integral, $H_{\ell di}$, and the empirical CPT criteria, $H_{\ell c}$.

[f] Uniform beam distribution.

[g] Threshold dose not stated explicitly, or stated threshold was for a more sensitive end-point than used above.

[h] Estimated beam radius.

[i] A grade II epithelial lesion threshold dose (reference 7).

[j] Threshold dose from mean of damage levels 2 and 3 ($P\sqrt{t}$ = 10.3) (reference 39).

TABLE 2. STROMAL COLLAGEN SHRINKAGE OR OPACITIES FROM IR LASER EXPOSURE; EXPERIMENTAL EXPOSURE CONDITIONS, MODEL PREDICTIONS, AND ANSI STANDARDS. MODEL PREDICTIONS ARE MADE FOR A DEPTH OF 66 μm

Experimental Exposure Conditions					ANSI	Model Predictions[e]	
Exposure duration	Absorp. coeff.[a] (cm^{-1})	Beam radius[b] r(1/e) (cm)	Exper. thresh.[c] H_{sa} (J/cm^2)	Experimental references	Laser expos. stand.[d] H_{ANSI} (J/cm^2)	For H_{se} Peak temp. rise (^oC)	H_{sa} at r=0 (J/cm^2)
1.4 ns	937	0.475[f]	> 0.2	49,77,78	0.01	>4	>1.56
50 ns	12	0.028	45	41	1.00	129	9.28
100 ns	11190	0.300[g]	> 0.3	49,77,78	0.01	>5	>1.57
55 ms	937	0.200	3.6	51,54,71-74	0.27	56	1.74
70 ms	937	0.125[f]	1.2[h]	7	0.29	18	1.87
300 ms	937	0.300	6.9[i]	39,40	0.41	70	2.68
500 ms	937	0.265	12	27	0.47	123	3.24
1 s	937	0.300	12.6[i]	39,40	0.56	79	4.30
1 s	937	0.200	15	30	0.56	92	4.39
1 s	937	0.250[f]	15	20,21	0.56	98	4.22
3 s	937	0.075[f]	17	11	0.74	67	6.84
~600 s	937	0.520[f]	228	42	60.00	30	188
1800 s	937	0.520[f]	540	22	180.00	24	554

[a] From Rusk et al. (59) except 12 cm^{-1} (1.54 μm) from Boettner and Dankovic (6).

[b] Gaussian beam distribution, unless stated otherwise.

[c] Thresholds were not explicitly stated for stromal damage but were selected from description of exposure effects; see text.

[d] ANSI Z136.1-1976 (reference 2).

[e] H_{sa} is the average of threshold doses predicted via the adiabatic, H_{sac}, and nonadiabatic criteria, H_{snc}.

[f] Uniform beam distribution.

[g] Estimated beam radius.

[h] A grade III lesion (reference 7).

[i] Threshold dose from mean of damage levels 3 and 4 ($P\sqrt{t}$ = 12.6) (reference 39).

TABLE 3. EPITHELIAL VAPORIZATION OR CORNEAL PERFORATION FROM IR LASER EXPOSURE: EXPERIMENTAL EXPOSURE CONDITIONS, MODEL PREDICTIONS, AND ANSI STANDARDS. MODEL PREDICTIONS ARE MADE FOR A DEPTH OF 6 μm

Experimental Exposure Conditions					ANSI	Model Predictions[e]	
					Laser expos. stand.[d]	For H_{ve} Peak temp.	
Exposure duration	Absorp. coeff.[a] (cm^{-1})	Beam radius[b] r(1/e) (cm)	Exper. thresh.[c] H_{ve} (J/cm^2)	Experimental references	H_{ANSI} (J/cm^2)	rise (°C)	H_{va} at r=0 (J/cm^2)
300 ms	937	0.300	17[f]	39,40	0.41	230	27
1 s	937	0.300	31[f]	39,40	0.56	230	48
1 s	937	0.250[g]	51	20,21	0.56	380	47
3 s	937	0.075[g]	85	11	0.74	360	80
4 s	937	0.200	48	30	0.79	280	59

[a]From Rusk et al. (59).

[b]Gaussian beam distribution, unless stated otherwise.

[c]Thresholds were not stated explicitly for epithelial vaporization or corneal perforation but were selected from description of exposure effects; see text.

[d]ANSI Z136.1-1976 (reference 2).

[e]H_{va} is the average of threshold doses predicted via the adiabatic, H_{vac}, and nonadiabatic criteria, H_{vnc}.

[f]A grade V lesion threshold (reference 39).

[g]Uniform beam distribution.

TABLE 4. LASERS, WAVELENGTHS AND ASSOCIATED ABSORPTION COEFFICIENTS USED FOR THE EXPERIMENTAL EXPOSURES (SEE TABLES 1-3).

Absorption coefficient[a] (cm^{-1})	Laser	Wavelength (μm)
11.9	Er	1.54
197[b]	DF	3.55-3.98
202[b]	DF	3.70-3.73
937	CO_2	10.6
1299	HF	2.727
3220[b]	HF	2.61-2.87
4906	HF	2.795
11190	HF	2.9

[a]From Palmer and Williams (50) for $\lambda<2.6$ μm, Rusk et al. (59) for $\lambda>2.6$ μm, except $\lambda = 1.54$ μm from Boettner and Dankovic (6).

[b]An average of a multiline spectrum weighted per spectral energy.

TABLE 5. ANATOMICAL AND THERMAL PROPERTIES FOR THE OCULAR MEDIA

Thicknesses of the Ocular Media[a]

Tear layer	6 μm
Cornea	0.05 cm
Aqueous	0.29 cm
Lens	0.35 cm
Vitreous	1.16 cm

Thermal Properties

Thermal conductivity[a]: 0.0012 cal/cm-sec-°C
Heat capacity: 1.0 cal/cm^3-°C
Normal corneal temperature[b]: 35°C
Collagen melting temperature[c]: 56°C
Collagen latent heat of transformation (solid to liquid)[d]: 25 cal/g or 5 cal/cm^3 in the stroma.
Water latent heat of transformation (liquid to gas): 539 cal/g or 539 cal/cm^3

Damage Criteria

Coefficients for damage integral[a] (epithelial lesion)
For T<323°K
C1 = 4.322×10^{64}/sec: lnC1 = 149
C2 = 50,000°K

For T>323°K
C1 = 9.389×10^{104}/sec: lnC1 = 242
C2 = 80,000°K

Critical Peak Temperatures (CPT) on beam axis

Empirical, epithelial lesion: $CPT = 79.6t^{-0.0152}$

Nonadiabatic:
- Stromal collagen: 61°C (at z = 66 μm)
- Epithelial steam: 639°C (at z = 6 μm)

Adiabatic:
- Stromal collagen: 56°C and 5 cal/g (at z = 66 μm)
- Steam: 100°C and 539 cal/g (at z = 6 μm)

---

[a]Takata et al. (69), pp. 25, 33, 34.

[b]Mikesell (45) unpublished data, Freeman and Fatt (25).

[c]Stringer and Parr (65).

[d]Gustavson (32); Prince (56) p. 98; Garrett and Flory (28).

TABLE 6. EMPIRICAL CRITICAL PEAK TEMPERATURE, CPT, AND TEMPERATURE RISES, ΔT, FOR MINIMUM EPITHELIAL LESIONS AT (r, z) = (0,6 μm)

CPT(°C):	105	98	92	85	80	74
ΔT(°C):	70	63	57	50	45	39
t(sec):	10^{-8}	10^{-6}	10^{-4}	10^{-2}	1.0	10^{2}

TABLE 7. EMPIRICAL THRESHOLD PEAK TEMPERATURE, TPT, AND TEMPERATURE RISES, ΔT, FOR MINIMUM EPITHELIAL LESIONS AT (r, z) = (0.76σ, 6 μm).

TPT(°C):	76	72	68	65	61	58
ΔT(°C):	41	37	33	30	26	23
t(sec):	10^{-8}	10^{-6}	10^{-4}	10^{-2}	1.0	10^{2}

TABLE 8. COMPARISON OF THEORETICAL AND EXPERIMENTAL THRESHOLDS AND ANSI STANDARDS: MINIMUM EPITHELIAL LESIONS[a]

	Relative lesion radius	$\frac{\Delta T(\bar{r}_\ell)}{\Delta T(0)}$	$\frac{H_{\ell di}(0)}{H_{\ell di}(\bar{r}_\ell)}$	$\frac{H_{\ell c}(0)}{H_{\ell di}(0)}$	$\frac{H_{\ell di}(r_\ell)}{H_{\ell e}}$	$\frac{H_{\ell a}}{H_{\ell e}}$	$\frac{H_{\ell e}}{H_{ANSI}}$[b]
Mean	0.76	0.56	0.59	1.74	1.03	0.83	9.6
90% conf.	0.70	0.50	0.44	1.66	0.56	0.74	2.0
interval	0.82	0.62	0.79	1.82	1.90	0.93	45.8
n	30	35	35	35	35	35	35

[a]The ratios of temperature rises, ΔT, and radiant exposure for minimum lesion thresholds, H_ℓ, are denoted as a function of radial position (i.e., $r = 0$ or $r = \bar{r}_\ell$, the mean relative lesion radius).

The other subscripts on H_ℓ define its derivation: di, from the damage integral; c, from the empirical critical peak temperature (CPT); e, from experimental data; and a, from the average of $H_{\ell di}$ and $H_{\ell c}$.

H_{ANSI} is the maximum permissible exposure level from ANSI Z136.1-1976 (reference 2).

[b]Ratios ranged from 2 to 151, and 9 of these were less than 5.0.

TABLE 9. COMPARISON OF THEORETICAL AND EXPERIMENTAL THRESHOLDS AND ANSI STANDARDS: STROMAL COLLAGEN SHRINKAGE[a]

	$\frac{H_{snc}}{H_{sac}}$	$\frac{H_{sa}}{H_{se}}$	$\frac{H_{se}}{H_{ANSI}}$	$\frac{H_{se}}{H_{\ell e}}$
Mean	1.2	0.4	14.2	1.7
90% conf.	0.9	0.1	2.6	1.4
interval	1.5	1.4	76.1	2.0
n	3	11	11	9

[a]The radiant exposure for stromal collagen shrinkage thresholds, H_s, have additional subscripts to define its derivation: nc, from the nonadiabatic critical peak temperature (CPT); ac, from the adiabatic CPT; e, from the experimental data; and a, from the average of H_{snc} and H_{sac}.

H_{ANSI} is the maximum permissible exposure level from ANSI Z136.1-1976 (reference 2).

$H_{\ell e}$ is the experimental lesion threshold radiant exposure.

TABLE 10. COMPARISON OF THEORETICAL AND EXPERIMENTAL THRESHOLDS AND ANSI STANDARDS: EPITHELIAL VAPORIZATION[a]

	$\frac{H_{vnc}}{H_{vac}}$	$\frac{H_{va}}{H_{ve}}$	$\frac{H_{ve}}{H_{\ell e}}$	$\frac{H_{ve}}{H_{ANSI}}$
Mean	6.2	1.2	4.0	68
90% conf.	5.5	0.9	1.7	28
interval	7.0	1.6	9.6	162
n	5	5	5	5

[a]The radiant exposure for epithelial vaporization thresholds, H_v, have additional subscripts to define its derivation: nc, from the nonadiabatic critical peak temperature (CPT); ac, from the adiabatic CPT; e, from the experimental data; and a, from the average of H_{vnc} and H_{vac}.

H_{ANSI} is the maximum permissible exposure level from ANSI Z136.1-1976 (reference 2).

$H_{\ell e}$ is the experimental lesion threshold radiant exposure.

TABLE 11. AVERAGE THRESHOLD RADIANT EXPOSURE FOR MINIMUM EPITHELIAL LESIONS, $H_{\ell a}$ (J/cm^2) [BEAM RADIUS (1/e) = 0.0707 cm, (r, z) = (0, 6 μm)].

Absorp. coeff. (cm^{-1})	Exposure duration (sec)					
	1.00E-08	1.00E-06	1.00E-04	1.00E-02	1.00E+00	1.00E+02
0.7	2.17E+02	2.01E+02	1.86E+02	1.96E+02	3.16E+02	4.55E+03
1.2	1.58E+02	1.47E+02	1.36E+02	1.29E+02	1.64E+02	2.03E+03
4.8	4.00E+01	3.71E+01	3.45E+01	3.35E+01	4.57E+01	7.25E+02
11.0	1.48E+01	1.38E+01	1.33E+01	1.43E+01	2.30E+01	4.91E+02
21.0	9.30E+00	8.66E+00	8.14E+00	8.33E+00	1.52E+01	3.85E+02
27.0	6.88E+00	6.40E+00	6.15E+00	6.39E+00	1.30E+01	3.54E+02
41.0	4.39E+00	4.12E+00	3.94E+00	4.29E+00	1.04E+01	3.17E+02
121.0	1.97E+00	1.82E+00	1.71E+00	1.91E+00	7.33E+00	2.71E+02
150.0	1.58E+00	1.49E+00	1.41E+00	1.64E+00	6.92E+00	2.61E+02
200.0	1.25E+00	1.16E+00	1.07E+00	1.35E+00	6.63E+00	2.56E+02
300.0	9.00E-01	8.31E-01	7.99E-01	1.09E+00	6.42E+00	2.53E+02
400.0	6.92E-01	6.47E-01	6.14E-01	9.34E-01	6.12E+00	2.46E+02
577.0	5.33E-01	4.97E-01	4.73E-01	8.23E-01	6.00E+00	2.43E+02
700.0	4.67E-01	4.40E-01	4.20E-01	7.76E-01	5.93E+00	2.41E+02
817.0	4.28E-01	3.98E-01	3.82E-01	7.45E-01	5.90E+00	2.41E+02
1000.0	3.96E-01	3.70E-01	3.52E-01	7.31E-01	5.88E+00	2.41E+02
1760.0	3.06E-01	2.87E-01	2.76E-01	6.55E-01	5.79E+00	2.38E+02
2000.0	2.94E-01	2.75E-01	2.65E-01	6.48E-01	5.77E+00	2.38E+02
2500.0	2.85E-01	2.65E-01	2.58E-01	6.47E-01	5.79E+00	2.39E+02
3038.0	2.86E-01	2.67E-01	2.58E-01	6.52E-01	5.84E+00	2.41E+02
4000.0	2.70E-01	2.52E-01	2.43E-01	6.31E-01	5.76E+00	2.37E+02
4920.0	2.73E-01	2.55E-01	2.46E-01	6.40E-01	5.84E+00	2.40E+02
6000.0	2.73E-01	2.55E-01	2.46E-01	6.40E-01	5.84E+00	2.40E+02
8000.0	2.72E-01	2.55E-01	2.46E-01	6.39E-01	5.83E+00	2.39E+02
12395.0	2.69E-01	2.53E-01	2.44E-01	6.33E-01	5.79E+00	2.38E+02

TABLE 12. AVERAGE THRESHOLD RADIANT EXPOSURE FOR STROMAL COLLAGEN SHRINKAGE, H_{sa} (J/cm^2) [BEAM RADIUS (1/e) = 0.0707 cm, (r, z) = (0, 66 μm); THE ADIABATIC THRESHOLDS WERE ESTIMATED FOR VALUES BELOW THOSE WITH AN ASTERISK, AS DESCRIBED IN PROCEDURES].

Absorp coeff (cm^{-1})	Exposure duration (sec)					
	1.00E-08	1.00E-06	1.00E-04	1.00E-02	1.00E+00	1.00E+02
0.7	1.55E+02	1.55E+02	1.55E+02	1.55E+02	2.29E+02	3.78E+03
1.2	9.26E+01	9.26E+01	9.26E+01	9.26E+01	1.20E+02	1.69E+03
4.8	2.37E+01	2.37E+01	2.37E+01	2.37E+01	3.41E+01	6.04E+02
11.0	1.07E+01	1.07E+01	1.07E+01	1.08E+01	1.68E+01	4.08E+02
21.0	5.93E+00	5.93E+00	5.93E+00	5.95E+00	1.09E+01	3.25E+02
27.0	4.81E+00	4.81E+00	4.81E+00	4.84E+00	9.34E+00	2.99E+02
41.0	3.46E+00	3.46E+00	3.46E+00	3.48E+00	7.54E+00	2.68E+02
121.0	1.90E+00	1.90E+00	1.90E+00	1.93E+00	5.51E+00	2.34E+02
150.0	1.79E+00	1.79E+00	1.79E+00	1.79E+00	5.25E+00	2.27E+02
200.0	1.64E+00	1.64E+00	1.64E+00	1.64E+00	5.11E+00	2.24E+02
300.0	1.59E+00	1.59E+00	1.59E+00	1.59E+00	5.10E+00	2.24E+02
400.0	1.53E+00 *	1.53E+00 *	1.53E+00 *	1.55E+00	5.04E+00	2.20E+02
577.0	1.53E+00	1.53E+00	1.53E+00	1.52E+00 *	5.00E+00	2.20E+02
700.0	1.53E+00	1.53E+00	1.53E+00	1.52E+00	5.02E+00 *	2.20E+02
817.0	1.53E+00	1.53E+00	1.53E+00	1.52E+00	5.02E+00	2.19E+02 *
≥ 1000.0	1.53E+00	1.53E+00	1.53E+00	1.52E+00	5.02E+00	2.19E+02

TABLE 13. AVERAGE THRESHOLD RADIANT EXPOSURES FOR EPITHELIAL VAPORIZATION, H_{va} (J/cm^2)
[BEAM RADIUS (1/e) = 0.0707 cm, (r, z) = (0, 6 μm); THE ADIABATIC THRESHOLDS WERE ESTIMATED FOR VALUES BELOW THOSE WITH AN ASTERISK, AS DESCRIBED IN PROCEDURES].

Absorp coeff (cm^{-1})	Exposure duration (sec)					
	1.00E-08	1.00E-06	1.00E-04	1.00E-02	1.00E+00	1.00E+02
0.7	2.48E+03	2.48E+03	2.48E+03	2.78E+03	4.00E+03	5.45E+04
1.2	1.93E+03	1.93E+03	1.93E+03	1.96E+03	2.39E+03	2.47E+04
4.8	4.65E+02	4.65E+02	4.65E+02	4.86E+02	6.31E+02	8.73E+03
11.0	1.57E+02	1.57E+02	1.58E+02	1.79E+02	2.84E+02	5.85E+03
21.0	1.04E+02	1.04E+02	1.04E+02	1.12E+02	1.88E+02	4.63E+03
27.0	7.52E+01	7.52E+01	7.55E+01	8.39E+01	1.54E+02	4.25E+03
41.0	4.77E+01	4.77E+01	4.80E+01	5.47E+01	1.18E+02	3.80E+03
121.0	2.30E+01*	2.30E+01*	2.30E+01	2.61E+01	8.08E+01	3.23E+03
150.0	1.86E+01	1.86E+01	1.87E+01*	2.17E+01	7.50E+01	3.12E+03
200.0	1.44E+01	1.44E+01	1.44E+01	1.75E+01	7.04E+01	3.05E+03
300.0	1.03E+01	1.03E+01	1.04E+01	1.35E+01	6.65E+01	3.03E+03
400.0	7.97E+00	7.97E+00	8.15E+00	1.13E+01	6.25E+01	2.93E+03
577.0	6.10E+00	6.10E+00	6.22E+00	9.41E+00	6.07E+01	2.90E+03
700.0	5.36E+00	5.36E+00	5.48E+00	8.73E+00	5.97E+01	2.88E+03
817.0	4.87E+00	4.87E+00	5.00E+00	8.25E+00	5.92E+01	2.87E+03
1000.0	4.48E+00	4.48E+00	4.60E+00	7.95E+00	5.80E+01	2.84E+03
1760.0	3.47E+00	3.47E+00	3.59E+00	7.13E+00*	5.77E+01*	2.84E+03
2000.0	3.35E+00	3.35E+00	3.47E+00	7.07E+00	5.74E+01	2.84E+03*
2500.0	3.23E+00	3.23E+00	3.37E+00	7.07E+00	5.74E+01	2.84E+03
3038.0	3.23E+00	3.23E+00	3.37E+00	7.07E+00	5.74E+01	2.84E+03
4000.0	3.05E+00	3.05E+00	3.18E+00	6.95E+00	5.74E+01	2.83E+03
4920.0	3.05E+00	3.05E+00	3.18E+00	6.95E+00	5.74E+01	2.83E+03
6000.0	3.05E+00	3.05E+00	3.18E+00	6.95E+00	5.74E+01	2.83E+03
8000.0	3.05E+00	3.05E+00	3.18E+00	6.95E+00	5.74E+01	2.83E+03
12395.0	3.05E+00	3.05E+00	3.18E+00	6.95E+00	5.74E+01	2.83E+03

TABLE 14. AVERAGE THRESHOLD RADIANT EXPOSURE FOR MINIMUM EPITHELIAL LESIONS, $H_{\ell a}$ (J/cm^2) [ABSORPTION COEFFICIENT = 817 cm^{-1}, (r, z) = (0, 6 μm)].

Beam radius 1/e (cm)	Exposure duration (sec)							
	1.00E-08	1.00E-06	1.00E-05	1.00E-04	1.00E-03	1.00E-02	1.00E+00	1.00E+02
0.0010	4.43E-01	4.16E-01	4.05E-01	4.58E-01	9.65E-01	5.42E+00	3.78E+02	3.05E+04
0.0100	4.31E-01	4.02E-01	3.89E-01	3.98E-01	4.40E-01	8.20E-01	2.17E+01	1.61E+03
0.0350	4.31E-01	3.98E-01	3.88E-01	4.06E-01	4.37E-01	7.65E-01	8.33E+00	4.80E+02
0.0707	4.24E-01	3.99E-01	3.86E-01	3.96E-01	4.33E-01	7.44E-01	5.90E+00	2.41E+02
0.1250	4.24E-01	3.99E-01	3.86E-01	3.96E-01	4.35E-01	7.48E-01	5.31E+00	1.60E+02
0.3000	4.29E-01	4.01E-01	3.86E-01	3.96E-01	4.34E-01	7.43E-01	4.86E+00	7.45E+01
1.0000	4.29E-01	4.01E-01	3.87E-01	3.97E-01	4.19E-01	7.46E-01	4.81E+00	4.71E+01

TABLE 15. AVERAGE THRESHOLD RADIANT EXPOSURE FOR STROMAL COLLAGEN SHRINKAGE, H_{sa} (J/cm^2) [ABSORPTION COEFFICIENT = 817 cm^{-1}, (r, z) = (0, 66 μm), THE ADIABATIC THRESHOLDS WERE ESTIMATED FOR VALUES BELOW THOSE WITH AN ASTERISK, AS DESCRIBED IN PROCEDURES].

Beam radius 1/e (cm)	Exposure duration (sec)							
	1.00E-08	1.00E-06	1.00E-05	1.00E-04	1.00E-03	1.00E-02	1.00E+00	1.00E+02
0.0010	2.81E+01*	2.88E+01*	2.81E+01*	3.04E+01	4.45E+01	5.74E+01	1.54E+03	1.42E+05
0.0100	2.04E+00	2.07E+00	2.04E+00	2.09E+00*	2.09E+00*	2.10E+00*	2.78E+01*	2.17E+03
0.0350	1.59E+00	1.59E+00	1.59E+00	1.59E+00	1.59E+00	1.60E+00	7.85E+00	4.75E+02
0.0707	1.55E+00	1.52E+00	1.51E+00	1.53E+00	1.52E+00	1.53E+00	5.25E+00	2.22E+02
0.1250	1.55E+00	1.52E+00	1.51E+00	1.53E+00	1.52E+00	1.53E+00	4.55E+00	1.37E+02
0.3000	1.55E+00	1.52E+00	1.51E+00	1.53E+00	1.52E+00	1.54E+00	4.16E+00	6.59E+01
1.0000	1.54E+00	1.53E+00	1.52E+00	1.51E+00	1.50E+00	1.53E+00	4.08E+00	4.17E+01

TABLE 16. AVERAGE THRESHOLD RADIANT EXPOSURE FOR EPITHELIAL VAPORIZATION, H_{va} (J/cm^2) [ABSORPTION COEFFICIENT = 817 cm^{-1}, (r, z) = (0, 6 μm)]

Beam radius 1/e (cm)	Exposure duration (sec)							
	1.00E-08	1.00E-06	1.00E-05	1.00E-04	1.00E-03	1.00E-02	1.00E+00	1.00E+02
0.0010	4.90E+00	4.92E+00	4.96E+00	5.40E+00	9.53E+00	4.71E+01	3.75E+03	3.68E+05
0.0100	4.90E+00	4.91E+00	4.91E+00	5.03E+00	5.65E+00	8.89E+00	2.15E+02	1.94E+04
0.0350	4.96E+00	4.90E+00	4.90E+00	5.09E+00	5.61E+00	8.42E+00	8.26E+01	5.72E+03
0.0707	4.87E+00	4.88E+00	4.87E+00	5.00E+00	5.59E+00	8.25E+00	5.92E+01	2.87E+03
0.1250	4.87E+00	4.88E+00	4.87E+00	5.00E+00	5.59E+00	8.25E+00	5.28E+01	1.80E+03
0.3000	4.87E+00	4.88E+00	4.87E+00	5.00E+00	5.59E+00	8.25E+00	4.85E+01	8.79E+02
1.0000	4.87E+00	4.88E+00	4.88E+00	5.00E+00	5.40E+00	8.25E+00	4.78E+01	5.48E+02

TABLE 17. RELATIVE THRESHOLD SENSITIVITY FOR PRINCIPAL LASER WAVELENGTHS IN THE 1.4 TO 1000 μm WAVELENGTH RANGE FOR EXPOSURES $\leq 10^{-4}$ SEC [BEAM RADIUS (1/e) = 0.0707 cm]

LASER	Er	Hol	HF	DF	CO	CO_2
λ (μm)	1.54	2.06	2.5-3.0	3.5-4.0	≈5	10.6
$\alpha(cm^{-1})$	≈11	41	121-12395	400-150	400-200	≈1000
			Minimum Epithelial Lesions			
	0.02	0.06	0.14-1.00	0.38-0.17	0.38-0.22	0.67
			Stromal Collagen Shrinkage			
	0.14	0.45	0.83-1.00	1.00-0.83	1.00-0.91	1.00
			Epithelial Vaporization			
	0.02	0.08	0.18-1.00	0.48-0.22	0.48-0.29	0.77

TABLE 18. SAFETY MARGINS OF CORNEAL SAFETY STANDARDS GIVEN AS RATIOS OF AVERAGE THRESHOLD PREDICTIONS AND ANSI STANDARDS (2). [BEAM RADIUS (1/e) = 0.0707 cm. VALUES FOR 11 cm^{-1} WOULD BE DIVIDED BY 100 if λ = 1.54 μm].

Absorp coeff (cm^{-1})	Exposure duration (sec)					
	10^{-8}	10^{-6}	10^{-4}	10^{-2}	1.0	10^{2}
			Minimum Epithelial Lesions			
4.8	4000	2100	616	190	82	72
11	1480	781	238	80	41	49
41	439	233	70	24	19	32
200	125	65	19	7.6	12	26
1000	40	21	6.3	4.1	10	24
12395	27	14	4.4	3.6	10	24
			Stromal Collagen Shrinkage			
4.8	2420	1370	432	137	62	62
11	1100	620	196	62	31	42
41	354	200	63	20	14	27
200	170	96	30	9.6	9.3	23
1000	159	90	28	9.0	9.3	23
12395	159	90	28	9.0	9.2	23
			Epithelial Vaporization			
4.8	46500	26200	8300	2750	1130	873
11	15700	8880	2820	1010	506	585
41	4770	2700	857	309	211	380
200	1440	812	258	99	126	305
1000	448	253	82	45	104	284
12395	305	172	57	39	103	283
H_{ANSI} (J/cm^2)	0.01	0.0178	0.056	0.177	0.56	10

TABLE 19. SAFETY MARGINS OF CORNEAL SAFETY STANDARDS GIVEN AS RATIOS OF AVERAGE THRESHOLD PREDICTIONS AND ANSI STANDARDS (2).
[ABSORPTION COEFFICIENT = 817 cm^{-1}]

Beam radius (1/e) (cm)	Exposure duration (sec)					
	10^{-8}	10^{-6}	10^{-4}	10^{-2}	1.0	10^{2}
			Minimum Epithelial Lesions			
0.001	44	24	8.2	31	675	3050
0.01	43	23	7.1	4.6	39	161
0.07	42	23	7.1	4.2	11	24
1.0	43	23	7.1	4.2	8.6	47
			Stromal Collagen Shrinkage			
0.001	2860	1660	553	331	2810	14500
0.01	212	122	39	12	52	249
0.07	161	89	28	9.0	9.7	25
1.0	160	90	28	9.0	7.6	4.5
			Epithelial Vaporization			
0.001	490	278	96	266	6690	36800
0.01	490	277	90	50	383	1940
0.07	487	276	89	47	106	287
1.0	487	276	89	47	85	55
H_{ANSI} (J/cm^2)	0.01	0.177	0.056	0.177	0.56	10